Cell Stem Cell

Article

Exploring the human lacrimal gland using organoids and single-cell sequencing

Graphical Abstract

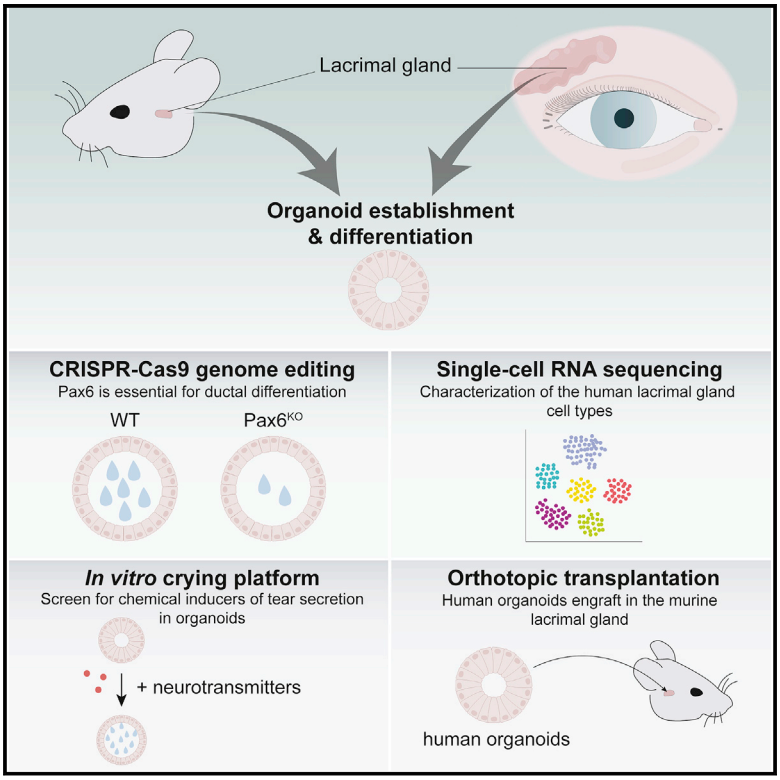

Highlights

- Derivation of adult stem cell-based organoids from mouse and human lacrimal gland
- Pax6 is essential to maintain lacrimal gland duct identity in adult cells
- Single-cell transcriptome analysis of major human lacrimal gland cell types
- Lacrimal gland organoids can be induced to cry and are transplantable

Authors

Marie Bannier-Hélaouët, Yorick Post, Jeroen Korving, ..., Rachel Kalmann, Saskia M. Imhoff, Hans Clevers

Correspondence

h.clevers@hubrecht.eu

In brief

Lacrimal gland biology remains poorly understood. Here, we establish organoids from mouse and human lacrimal gland that can serve as study subjects for the lacrimal gland *in vitro*. In addition, we describe the human lacrimal gland at the single-cell level, which provides a platform for future studies.

Bannier-Hélaouët et al., 2021, Cell Stem Cell *28*, 1–12
July 1, 2021 © 2021 Elsevier Inc.
https://doi.org/10.1016/j.stem.2021.02.024

CellPress

Please cite this article in press as: Bannier-Hélaouët et al., Exploring the human lacrimal gland using organoids and single-cell sequencing, Cell Stem Cell (2021), https://doi.org/10.1016/j.stem.2021.02.024

Cell Stem Cell

CellPress

Article

Exploring the human lacrimal gland using organoids and single-cell sequencing

Marie Bannier-Hélaouët,[1,2,6] Yorick Post,[1,5,6] Jeroen Korving,[1,2] Marc Trani Bustos,[1] Helmuth Gehart,[1,3] Harry Begthel,[1,2] Yotam E. Bar-Ephraim,[1,2] Jelte van der Vaart,[1,2] Rachel Kalmann,[4] Saskia M. Imhoff,[4] and Hans Clevers[1,2,7,*]

[1]Hubrecht Institute, Royal Netherlands Academy of Arts and Sciences (KNAW), University Medical Center Utrecht, 3584 CT Utrecht, the Netherlands

[2]Oncode Institute, Hubrecht Institute, 3584 CT Utrecht, the Netherlands

[3]Institute for Molecular Health Sciences, ETH Zurich, 8093 Zurich, Switzerland

[4]Department of Ophthalmology, University Medical Center Utrecht, 3584 CX Utrecht, the Netherlands

[5]Present address: Surrozen, Inc., South San Francisco, CA 94080, USA

[6]These authors contributed equally

[7]Lead contact

*Correspondence: h.clevers@hubrecht.eu

https://doi.org/10.1016/j.stem.2021.02.024

SUMMARY

The lacrimal gland is essential for lubrication and protection of the eye. Disruption of lacrimal fluid production, composition, or release results in dry eye, causing discomfort and damage to the ocular surface. Here, we describe the establishment of long-term 3D organoid culture conditions for mouse and human lacrimal gland. Organoids can be expanded over multiple months and recapitulate morphological and transcriptional features of lacrimal ducts. CRISPR-Cas9-mediated genome editing reveals the master regulator for eye development *Pax6* to be required for differentiation of adult lacrimal gland cells. We address cellular heterogeneity of the lacrimal gland by providing a single-cell atlas of human lacrimal gland tissue and organoids. Finally, human lacrimal gland organoids phenocopy the process of tear secretion in response to neurotransmitters and can engraft and produce mature tear products upon orthotopic transplantation in mouse. Together, this study provides an experimental platform to study the (patho-)physiology of the lacrimal gland.

INTRODUCTION

Lacrimal glands are exocrine organs that secrete the aqueous layer of the tear film (Hodges and Dartt, 2003). Tears consist of water, mucins, lipids, electrolytes, and antibacterial proteins. Altogether, they lubricate and protect the eye from external insults (Hodges and Dartt, 2003). Most tear fluid is secreted by the epithelial cells of the main lacrimal glands, which consist of acini and intralobular ducts (Hodges and Dartt, 2003). In addition, myoepithelial cells encircle acini, but their precise function remains subject to further research (Makarenkova and Dartt, 2015). Tear secretion is mainly controlled by parasympathetic nerves, which secrete neurotransmitters such as acetylcholine and noradrenaline that trigger the release of tear components by acinar and ductal cells (Hodges and Dartt, 2016). Dysfunction in tear production or secretion potentially results in (or can be a consequence of) pathologies of the eye, such as dry eye disease or Sjögren's syndrome (Messmer, 2015; Brito-Zerón et al., 2016).

The regenerative capacity of the lacrimal gland during natural cell turnover and upon injury remains poorly understood, hampering the development of therapeutic options in dry eye pathologies. Recent data suggest that distinct progenitor cells exist for acinar and ductal cells and propose *Krt5* as a marker for ductal cell progenitors in mice (Farmer et al., 2017). To date, the expression of tear proteins in humans has been studied by mass spectrometry of tears from healthy and diseased individuals (Perumal et al., 2016) and by microarray of human lacrimal gland tissue (Turner et al., 2007). Therefore, the cellular heterogeneity of lacrimal gland epithelium, underlying the production of tear components, has remained largely unknown. While cultures of primary tear gland cells have been described, they are short-term (Lin et al., 2019), involve the use of poorly defined mesenchymal stem cells (Massie et al., 2018), expand on a serum-based growth medium (Tiwari et al., 2012), are derived from embryonic material (Hirayama et al., 2013), or solely work for mouse tissue (Xiao and Zhang, 2020). No long-term protocol for growing primary human tear gland cells currently exists.

Organoid technology has proven to faithfully recapitulate the structural and functional properties of multiple adult epithelial organs. Organoids derived from adult stem cells hold promise to model human tissue physiology, maintenance/repair, and disease (Clevers, 2016). The combination with single-cell sequencing technology of organoid cells and their corresponding tissue provides a robust experimental platform. Here, we establish lacrimal gland ductal organoids derived from murine and human tissue that engraft upon transplantation and swell upon stimulation by neurotransmitters. By single-cell mRNA sequencing of tissue and organoids, we uncover the cellular heterogeneity within the lacrimal gland.

Please cite this article in press as: Bannier-Hélaouët et al., Exploring the human lacrimal gland using organoids and single-cell sequencing, Cell Stem Cell (2021), https://doi.org/10.1016/j.stem.2021.02.024

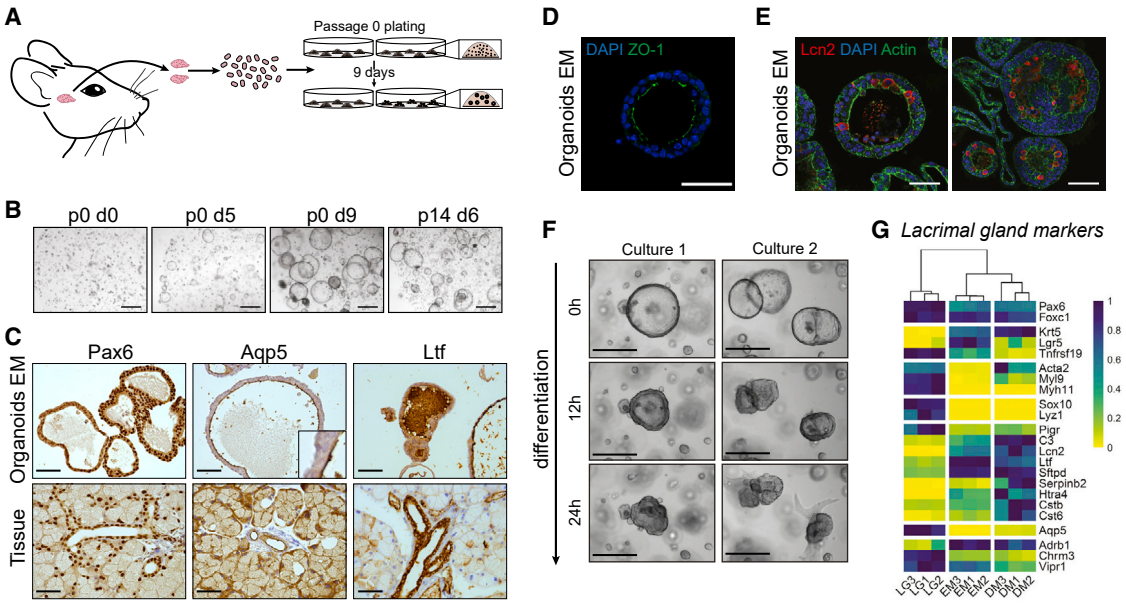

Figure 1. Establishment of organoid culture conditions for murine lacrimal gland

(A) Schematic representation of organoid derivation from murine lacrimal glands.

(B) Organoid outgrowth in BME from plating primary tissue to late passage. Scale bars, 500 μm.

(C) Immunohistochemistry for lacrimal gland markers Pax6, Aqp5, and Ltf in organoids under expansion conditions (expansion medium [EM]) and in tissue. Scale bars, 50 μm.

(D) Immunofluorescent staining for ZO-1 (green) in lacrimal gland organoids under expansion. Scale bar, 50 μm.

(E) Immunofluorescent staining for Lcn2 (red) and actin (green) in lacrimal gland organoids under expansion. Scale bars, 50 μm.

(F) Representative bright-field images of organoid morphology in differentiation medium (DM) over time. Scale bars, 200 μm.

(G) Heatmap indicating the expression of lacrimal gland markers in lacrimal gland tissue (LG) and organoids in expansion (EM) and differentiation (DM) conditions (linear scale).

See also Figure S1 and Table S1.

RESULTS

Establishment and differentiation of mouse lacrimal gland organoids

We have previously defined 3D culture conditions that allow long-term expansion of mouse and human organoids from multiple adult organs (Clevers, 2016). To generate lacrimal gland organoids, we evaluated our adult stem cell-based organoid protocols developed for other organs with mouse tissue (Sato et al., 2009; Drost et al., 2016; Hu et al., 2018; Schutgens et al., 2019). Wild-type murine lacrimal glands were minced, incubated in collagenase for 15 min, and embedded in basement membrane extract (BME) (Figure 1A). Supplying an organoid medium containing R-spondin 3, Noggin, FGF10, the transforming growth factor β (TGFβ) inhibitor A83-01, and the cyclic AMP (cAMP)/Protein kinase A (PKA) activators Prostaglandin E2 (PGE2) and Forskolin (FSK) resulted in the most robust organoid outgrowth (Figures S1A and S1B). Addition of nicotinamide slightly reduced initial outgrowth from primary tissue but is described to increase the lifespan of established organoids (Sato et al., 2011) and was therefore retained in the cocktail. Using this expansion medium (EM), organoids expanded to a diameter of ~200 μm within the first 10 days (Figure 1B). Thereafter, organoids could be passaged by mechanical disruption at a ratio of 1:4 every 7 days (to date until passage 40) without significant changes in growth kinetics, morphology, or general behavior (Figure 1B). By mapping protein expression using immunohistochemistry (IHC), we confirmed nuclear expression of transcription factor Pax6 in all organoid cells and in epithelial cells of the tissue (Figure 1C). *Pax6* is expressed in various tissues of the eye, including the lacrimal gland epithelium (Makarenkova et al., 2000). In both vertebrates and invertebrates, the master eye regulator Pax6 can induce the formation of ectopic eyes (Halder et al., 1995; Chow et al., 1999). In addition, we detected a polarized apical expression pattern of aquaporin 5 (Aqp5) in the organoids, similar to the apical marker ZO-1 (Figures 1C and 1D). The same expression pattern can be detected in the ducts and acini *in vivo* (Figure 1C). Defects in acinar cell apical distribution of AQP5 have been implicated in decreased lacrimation and dry eye in patients with Sjögren's syndrome (Tsubota et al., 2001). Lactotransferrin (Ltf), which has antimicrobial activity in various secretory fluids (Jenssen and Hancock, 2009), accumulated in the lumen of the organoids (Figure 1C). In mouse tissue, we found Ltf to be highly enriched in the ducts of the lacrimal gland (Figure 1C). Finally, the tear component lipocalin 2 (Lcn2), an iron-sequestering protein of the antibacterial innate immune response, accumulated in luminal cells of the organoids (Figure 1E).

We noticed that larger organoids collapsed into thicker-walled structures when fresh medium was not added frequently or when cultures were not split. This "differentiation" phenotype could be reproduced by withdrawal of most growth factors and small molecules (R-spondin, Noggin, A83-01, PGE2, nicotinamide, and

Please cite this article in press as: Bannier-Hélaouët et al., Exploring the human lacrimal gland using organoids and single-cell sequencing, Cell Stem Cell (2021), https://doi.org/10.1016/j.stem.2021.02.024

N-acetylcysteine) from EM for 5 days (Figure 1F). We termed this medium "differentiation medium" (DM).

To characterize the gene expression signature of the organoids as compared to the tissue, we performed bulk mRNA sequencing on organoids in EM (n = 3), organoids in DM (n = 3), and lacrimal gland tissue (n = 3) (Figure 1G). In culture, we noticed that upon differentiation, organoids became less proliferative and denser yet remained viable for multiple days, which was confirmed by the expression of cell-cycle-related genes in the dataset (Figure S1C). On the other hand, organoids cultured in EM displayed increased expression of stem cell markers, such as *Lgr5*, *Axin2*, *Tnfrsf19*, and *Krt5*, while organoids cultured in DM upregulated *Dkk3*, a Wnt pathway inhibitor (Figures 1G, S1D, and S1E; Table S1). Neither in EM nor in DM did the organoids express the acinar cell markers *Sox10* and *Lyz1*, suggesting that they did not contain acinar cells (Figure 1G) (Farmer et al., 2017). Upon differentiation, organoids upregulated the expression of the myoepithelial cell markers *Acta2* and *Myl9* (but not *Myh11*), markers of differentiated cells known from other tissues like the stomach (*Krt20*) (Stange et al., 2013), known tear products (*Pigr*, *C3*, *Lcn2*, *Ltf*, *Sftpd*, *Serpinb2*, *Serpinb5*, *Cstb*, and *Cst6*) (Dor et al., 2019; Vieira et al., 2017), and the water channel *Aqp5* (Figures 1G, S1D, and S1G; Table S1). Gene Ontology (GO) term enrichment analysis revealed that genes involved in immune defense response were also upregulated in DM (Figure S1F). In addition, the expression of genes encoding the human tear proteome (Dor et al., 2019) was higher in mouse organoids when cultured in DM (Figure S1H). Retinol production is an important function of the lacrimal gland, as retinol promotes healing and differentiation of the cornea (Samarawickrama et al., 2015). Lacrimal gland organoids expressed a range of enzymes involved in retinol metabolism; in EM, the expression of *Rdh16* and *Adh6a* was highest, while *Rdh10* and *Aldh1a3* were elevated in DM (Figure S1D). Retinol, protein, and water secretions by the lacrimal gland are tightly controlled by sympathetic and parasympathetic stimulation (Dartt, 2009). Organoids retained the expression of important receptors for neurotransmitter signal transduction (*Adrb1*, *Chrm3*, and *Vipr1*) (Figure 1G). Lastly, organoids upregulated genes involved in exocytosis (*Rab27b* and *Rab31*) upon differentiation (Figure S1D). Taken together, DM conditions promote ductal cell maturation by inducing the expression of a broad range of tear products.

Role of Pax6 in lacrimal gland homeostasis

The transcription factor Pax6 is indispensable for lacrimal gland development in mouse (Makarenkova et al., 2000), and its overexpression is pivotal in the generation of lacrimal gland epithelium-like cells from human pluripotent stem cells (Hirayama et al., 2017). To decipher its role in adult murine lacrimal gland cells, we utilized CRISPR-Cas9 technology for targeted deletion of *Pax6* in our organoids (Figure 2A). Clonally expanded knockout lines had undetectable levels of Pax6 protein by immunohistochemistry and western blot (Figures 2B and S2A). In EM, Pax6-knockout (Pax6-KO) lines were indistinguishable from their wild-type (WT) counterparts and maintained the growth speed, the cystic morphology and the capacity for repeated passaging (Figure 2C). We next tested the maturation capacity of Pax6-KO lines in response to DM. While WT lines became denser (as described above), Pax6-KO lines retained an undifferentiated cystic phenotype upon exposure to DM (Figure 2C). To investigate the gene expression changes occurring upon Pax6-KO, we performed bulk mRNA sequencing of the WT and Pax6-KO lines (n = 2 biological replicates each) cultured in EM or DM for 5 days. Upon differentiation, we observed that Pax6-KO organoids reduced their proliferation rate despite the unchanged morphology, which was corroborated by the expression of cell-cycle-related genes (Figure S2B). More importantly, we found 715 differentially expressed genes between WT and KO in EM and 513 in DM (fold change > 2, p-adjusted < 0.01) (Figures 2D, S2C, and S2D; Table S1). Among the genes downregulated in the Pax6-KO lines, we found receptors for neurotransmitters involved in the induction of lacrimal gland secretion, such as the muscarinic receptors *Chrm1* and *Chrm3*, the adrenergic receptor *Adrb1*, the purinergic receptors *P2ry2* and *P2ry6*, and the vasoactive intestinal peptide receptor *Vipr1* (Figures 2D, S2D, and S2E). Additionally, genes implicated in the secretion machinery were downregulated in Pax6-KO lines in EM and/or DM (Figures 2D and S2E). For instance, *Aqp5* was not upregulated upon differentiation in Pax6-KO as compared to WT, and Pax6-KO organoids had decreased levels of *Mlph*, *Myh10*, *Ank*, *Spire2*, and *Rab27a* that are involved in cytoskeleton remodeling and vesicle trafficking (Figures 2D, S2D, and S2E). Genes encoding common tear products, such as *Serpine2*, *Htra4*, or *Sftpd*, were downregulated in Pax6-KO lines in EM, and most remained low in DM (Figures 2D and S2C–S2E). Some genes involved in retinol metabolism that were enriched in EM in WT organoids (*Adh1*, *Adh6a*, *Adh7*, and *Rdh16*) were not expressed by Pax6-KO organoids, suggesting a reduction in retinol production by Pax6-KO lines (Figures 2D and S2C). Instead, GO term enrichment analysis of genes upregulated in differentiated Pax6-KO lines compared to WT revealed an increased response to interferon β (IFNβ) (Figure S2F). Furthermore, we found a large number of interferon response genes to be upregulated in expansion and in differentiation in Pax6-KO lines as compared to WT lines, suggesting Pax6-KO organoids are in a state of stress triggering an innate immune response (Figures S2C–S2E and S2G). Together, these data show that Pax6 is required for maintaining the expression of key genes for lacrimal gland functionality in expansion and differentiation conditions yet is dispensable for the expansion of ductal organoids.

Establishment and differentiation of human lacrimal gland organoids

We next pursued the establishment of human lacrimal gland organoids. Starting from surplus material from diagnostic lacrimal gland biopsies (n = 4), we adapted the mouse protocol to human tissue (Figures 3A and S3A). Plating of dissociated tissue fragments resulted in the initial expansion of human organoids within 9 days (Figure 3B). We observed optimal outgrowth and long-term expansion of cystic organoids in a medium containing R-spondin 3, Noggin, FSK, FGF10, N-acetylcysteine, and A83-01 (Figure S3B). Human organoids could be passaged by mechanical disruption at a ratio of 1:3 every 10 days, for multiple months (for at least 20 passages, n = 2 independent lines) without showing any sign of senescence or phenotypic change (Figure 3B). Immunohistochemistry confirmed the epithelial lacrimal gland identity of the organoids, matching the reference primary tissue by nuclear expression of PAX6 (Figure 3C). Additionally, all organoid cells were positive for epithelial cell

Please cite this article in press as: Bannier-Hélaouët et al., Exploring the human lacrimal gland using organoids and single-cell sequencing, Cell Stem Cell (2021), https://doi.org/10.1016/j.stem.2021.02.024

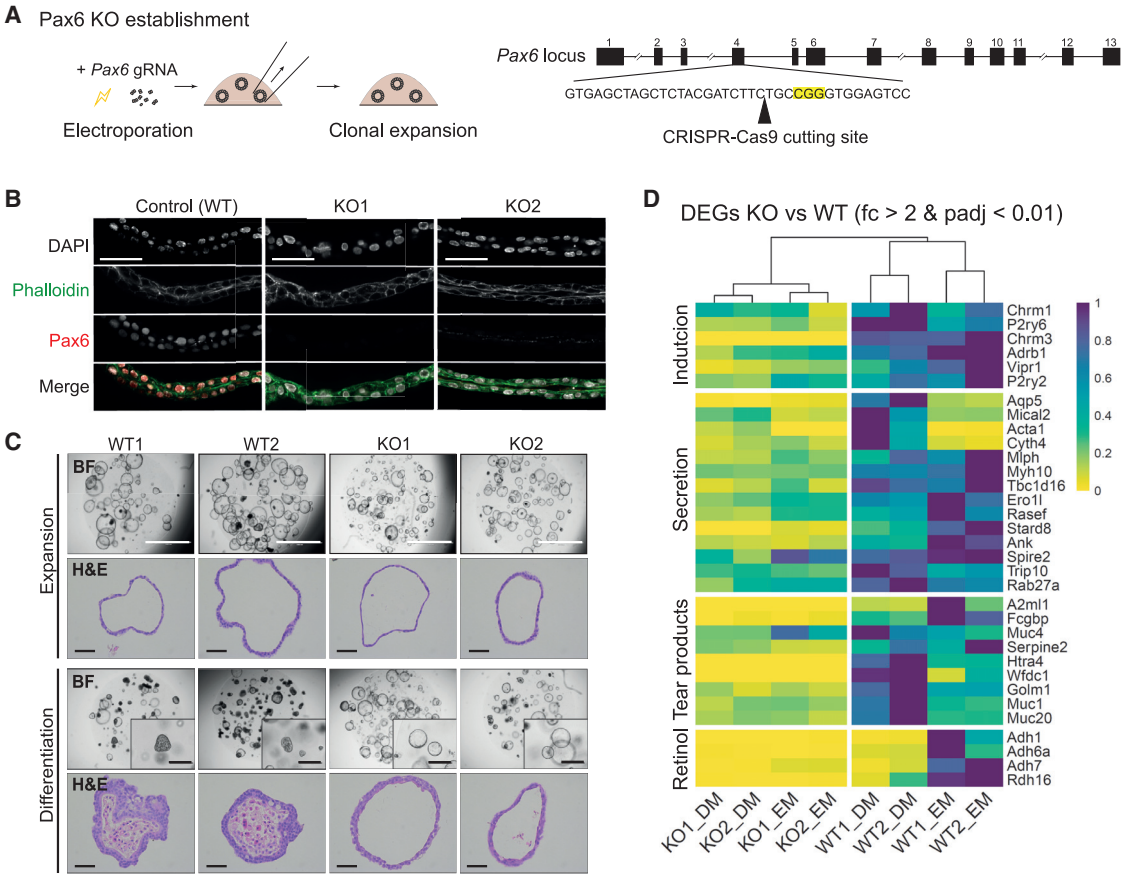

Figure 2. Lacrimal gland organoid differentiation requires *Pax6* expression

(A) Schematic representation of the targeting strategy for *Pax6* exon 4 using CRISPR-Cas9.

(B) Immunofluorescent staining for Pax6 protein in WT and KO lines. Scale bars, 50 μm.

(C) Bright-field (BF) images and H&E stainings of WT and KO lines in expansion and differentiation. Scale bars, 2 mm (BF) and 400 μm (BF zoom); H&E, 50 μm.

(D) Heatmap of a subset of differentially expressed genes between WT and KO under expansion (EM) and differentiation (DM) (fold change > 2, p-adjusted < 0.01, linear scale).

See also Figure S2 and Table S1.

adhesion molecule (EpCAM) (Figure S3C), while AQP5 was detected at the apical membrane, similar to murine organoids (Figure 3C).

To further improve the functionality of the organoids, we sought to differentiate them. After splitting, organoids were first cultured in human EM for 2 days and then transferred for 7 days to human DM (containing N-acetylcysteine and the Notch inhibitor DAPT). Upon exposure to human DM, organoids became denser yet retained a lumen (Figure 3D). Under expansion conditions, most cells expressed the basal cell marker TP63 (Figure 3E). TP63$^+$ basal cells persisted in human DM but remained restricted to the basal (outside) layer of the organoids (Figure 3E). Organoid differentiation was associated with a decrease of proliferation as indicated by a reduced number of KI67$^+$ cells when compared to organoids in EM (Figure 3F). Differentiation increased AQP5 expression (Figures 3F and S3D) and increased expression of myoepithelial cell markers (*ACTA2* and *KRT5*) (Figure S3D) and tear products (*LCN2*, *WFDC2*, *LYZ*, and *LTF*) (Figures 3G and S3D). Upon differentiation, protein accumulation inside the organoids could be detected for WFDC2 and LTF (Figures 3H and S3E). Importantly, differentiated organoids displayed increased expression of the muscarinic receptor *CHRM3* at levels close to primary lacrimal gland tissue (Figure 3G). In sum, human DM allows for the increased expression of tear products and several functional markers of lacrimation.

Single-cell characterization of human lacrimal gland tissue and organoids

In recent years, single-cell sequencing technologies have revealed the cellular composition of various human organs (Regev et al., 2017). To uncover the cellular heterogeneity of the lacrimal gland, we performed single-cell mRNA sequencing on primary human lacrimal gland tissue and organoids. First, a total of 1,533 tissue cells were sorted from three different tissue biopsies and processed using the SORT-seq method (Muraro et al., 2016). 916 cells with more than 1,500 unique transcript reads were separated into 17 different clusters, as visualized by Uniform Manifold Approximation and Projection (UMAP) embedding (Figures 4A and S4A; Table S2). Based on the expression of established markers, we identified 800 epithelial cells (*PAX6*,

Please cite this article in press as: Bannier-Hélaouët et al., Exploring the human lacrimal gland using organoids and single-cell sequencing, Cell Stem Cell (2021), https://doi.org/10.1016/j.stem.2021.02.024

CellPress

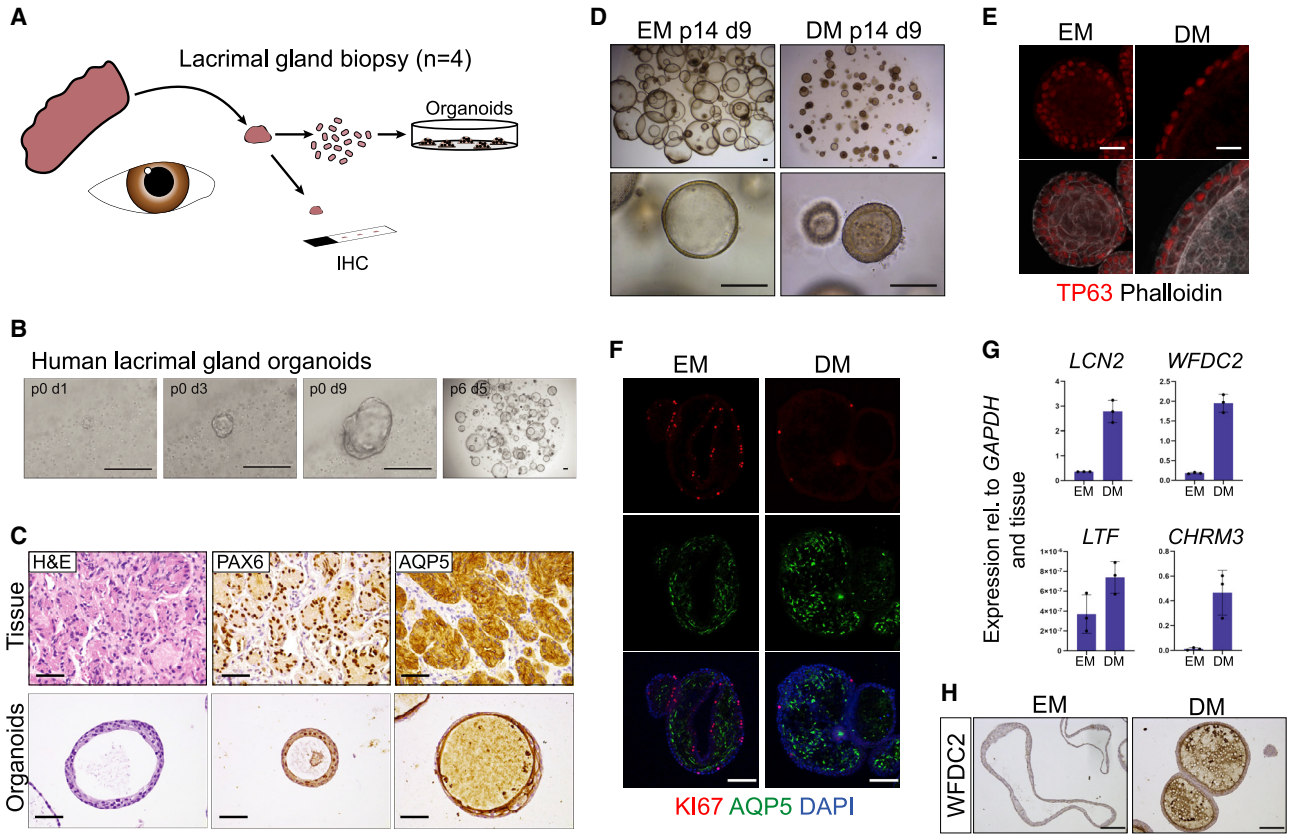

Figure 3. Establishment and differentiation of human lacrimal gland organoids

(A) Schematic representation of experimental setup for human lacrimal gland organoids and immunohistochemistry validation using biopsy samples. Organoids were derived from four samples with a 100% efficiency.

(B) Human organoid outgrowth from plating primary tissue to late passage. Scale bars, 200 μm.

(C) H&E, PAX6, and AQP5 staining in lacrimal gland tissue and organoids cultured in EM. Scale bars, 50 μm.

(D) Morphology of human organoids 9 days after the the begining of exposure to DM. Scale bars, 200 μm.

(E) Immunofluorescence staining for TP63 (red) and phalloidin (white) in organoids under expansion (EM) and differentiation (DM) conditions for 9 days. Scale bars, 25 μm.

(F) Staining for KI67 (red) and AQP5 (green) in human lacrimal gland organoids cultured in EM or DM for 9 days. Scale bars, 100 μm.

(G) qPCR analysis of the expression level of secreted tear products *LCN2*, *WFDC2*, and *LTF*, as well as of the muscarinic receptor *CHRM3*, in organoids cultured in EM or DM for 9 days. Each dot represents an independent experiment. Error bars indicate SEM.

(H) WFDC2 staining in human lacrimal gland organoids in expansion (EM) and differentiation (DM). Scale bars, 50 μm.

See also Figure S3.

FOXC1, and *AQP5*), 16 myoepithelial cells (*ACTA2*, *MYH11*, *MYLK*, and *TPM2*), 11 endothelial cells (*CDH5* and *PECAM1*), and 90 lymphocytes (*PTPRC* and *CD2*) (Figures S4B–S4E).

Epithelial cells in clusters 1, 2, 3, 4, 5, 6, 9, 11, 12, 13, 16, and 17 (n = 724) expressed high levels of *LTF*, *LCN1*, and *LYZ* (Figures 4B and S4F; Table S2). Protein staining on human lacrimal gland tissue revealed that, unlike in the mouse, antibacterial LTF was mainly present in the shape of granules in acinar cells. (Figure 4B). Likewise, LCN1 (a tear product against which antibodies have been found in patients with Sjögren's syndrome) and the antimicrobial LYZ were also expressed by most acinar cells (Figure S4F; Table S2) (Navone et al., 2005). In this large population of acinar cells, we identified subpopulations expressing high levels of other tear products. In clusters 1, 4, 5, 12, 16, and 17, we found the previously unidentified tear product *PRR27* to be enriched (Figure 4B; Table S2). In human lacrimal gland tissue, PRR27 only marked a subpopulation of acinar cells (Figure 4B). Among genes enriched in clusters 9 and 11, we found *LACRT*, which has antibacterial properties and promotes acinar cell secretion (Fujii et al., 2013; McKown et al., 2014); the secretoglobins *SCGB1D1* and *SCGB2A1*, also known as lipophilins A and C, which were previously identified in human tears (Lehrer et al., 1998); and the cystatins *CST1* and *CST4*, which are protease inhibitors (Figures 4B and S4G; Table S2). By protein staining, we confirmed that SCGB2A1 was also expressed by a subpopulation of acinar cells in the human lacrimal gland tissue (Figure 4B). In cluster 12, histatin *HTN1*, which displays antibacterial and wound-healing properties in saliva and has recently been identified in human tears, was enriched (Figure 4B; Table S2) (Torres et al., 2018; Kalmodia et al., 2019). We additionally confirmed by staining that HTN1 marked a subpopulation of acinar cells (Figure 4B). Lastly, in clusters 16 and 17, we identified *SMR3A*$^{+}$ acinar cells while, in cluster 13, we detected *SMR3B* to be enriched (Figures S4G and S4H; Table S2). Neither

Please cite this article in press as: Bannier-Hélaouët et al., Exploring the human lacrimal gland using organoids and single-cell sequencing, Cell Stem Cell (2021), https://doi.org/10.1016/j.stem.2021.02.024

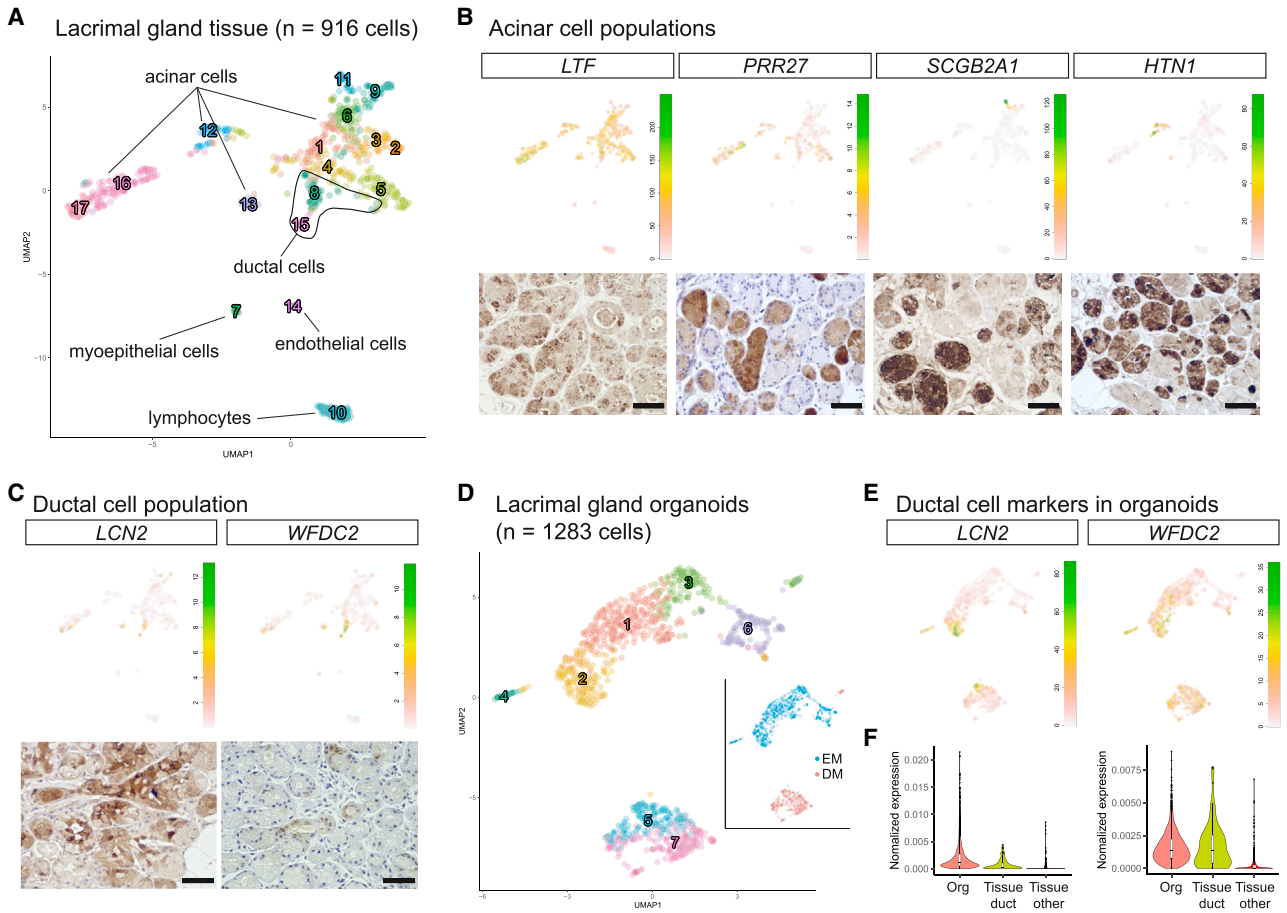

Figure 4. Characterization of human lacrimal gland tissue and organoids by single-cell mRNA sequencing

(A) UMAP representation of 18 clusters of human lacrimal gland tissue cells (n = 916) indicating major cell types.

(B) Top: UMAP representation of the expression of the acinar cell markers *LTF*, *PRR27*, *SCGB2A1*, and *HTN1* (linear scale). Bottom: corresponding stainings in the human lacrimal gland tissue. Scale bars, 50 μm.

(C) Top: UMAP representation of the expression of the ductal cell markers *LCN2* and *WFDC2* (linear scale). Bottom: corresponding stainings in the human lacrimal gland tissue. Scale bars, 50 μm.

(D) UMAP representation of 13 clusters of human lacrimal gland organoid cells (n = 1,283). The inset indicates the culturing conditions of the cells, with expansion (EM) in blue and differentiation (DM) in pink.

(E) UMAP representation of the expression of *LCN2* and *WFDC2* in the organoid dataset (linear scale).

(F) Violin plots of the normalized expression level of *LCN2* (left) and *WFDC2* (right) in organoid cells ("Org"; n = 1,283 cells), tissue cells from ductal origin ("Tissue duct," clusters 8 and 15 in A; n = 76 cells), and another origin ("Tissue other," all other clusters in A; n = 841 cells).

See also Figure S4 and Tables S3, S4, and S5.

have been identified in tears so far, but both have been reported in saliva before (Hay et al., 1988; Schlesinger et al., 1994). Importantly, the expression pattern of all these markers, at the RNA and protein levels, suggested that different tear products are produced by different acinar cell subpopulations.

Tissue clusters 8 and 15 (n = 76 cells) expressed high levels of *LCN2*, *WFDC2*, and C3 compared to acinar cells (Figures 4A, 4C, and S4I; Table S2). LCN2 is a known tear product with antibacterial properties that is involved in autoimmunity, WFDC2 belongs to a family of antibacterial peptides but has never been described in tears so far (Hua et al., 2014), and C3 is a complement factor whose activity in the tears has been extensively described (Willcox et al., 1997). When probing the expression of LCN2 and WFDC2 in human lacrimal gland tissue, we found that these genes were expressed by ductal cells (Figure 4C). Thus, ductal cells were transcriptionally different from acinar cells and expressed unique tear products.

To identify to which tissue cells the organoids were most similar, we also performed single-cell mRNA sequencing on organoids cultured in EM and DM. We sequenced a total of 960 cells in expansion and 576 in differentiation, out of which respectively 841 and 442 passed the threshold of 4,000 transcripts (Figure 4D). These 1,283 cells clustered into seven different clusters (Figure 4D; Table S3). *LCN2* was expressed by organoid clusters 2 and 5, while we found the tear product *WFDC2* to be enriched in clusters 1, 2, 5, and 7 (Figure 4E; Table S3). In primary tissue, both *LCN2* and *WFDC2* were expressed by ductal cells but had a much lower expression in other tissue cells, including in acinar

Please cite this article in press as: Bannier-Hélaouët et al., Exploring the human lacrimal gland using organoids and single-cell sequencing, Cell Stem Cell (2021), https://doi.org/10.1016/j.stem.2021.02.024

cells (Figures 4C and 4F; Table S2). In addition, the complement factor *C3* and the modulator of acetylcholine signaling *PSCA*, which were enriched in tissue ductal cells, were also broadly expressed by organoid cells (Figure S4I; Table S3) (Fu et al., 2015). Together, this implied that organoid cells represent ductal cells of the tissue.

Next, we sought to better characterize the differences between organoid cells cultured in EM and in DM (Figure S4J; Table S4). As anticipated, the basal cell marker *KRT5* was enriched in organoids under expansion in clusters 3 and 6 (Figures S4J and S4K; Table S4). In line with TP63 protein expression in organoids (Figure 3E), *KRT14*, *NGFR*, and *TP63* were highly expressed in these clusters (Figure S4K). These genes were also expressed by some ductal cells of tissue cluster 15 (Figure S4K; Table S2). Several tear products were enriched in EM compared to DM, such as *SCGB1A1*, the serine protease inhibitors *SERPINB1* and *SERPINB3*, and the antimicrobial product previously described in the upper airway *BPIFA1* (Figure S4J; Table S4) (Tsou et al., 2018). *BPIFA1* was expressed solely in organoid cluster 4, and we did not detect it in our tissue single-cell dataset. However, when we stained the human lacrimal gland tissue, we found it to be expressed by rare acinar cells (Figure S4L). Thus, our protocol might also sustain the expansion of rare acinar cells, yet this would require further validation. Upon differentiation, organoids expressed higher levels of the water channel *AQP5* (as observed by qPCR; Figure S3D), the coagulation factor *F3*, the secreted mucins *MUC16* and *MUC5AC*, and the immunoglobulin receptor *PIGR*, whose expression reached levels similar to primary tissue ductal cells (Figures S4J and S4M; Table S4). Finally, using single-cell RNA velocity, we confirmed a directional progression of transcriptional states across the organoid dataset, from *KRT5*$^{+}$ basal clusters 3 and 6 to *LCN2*$^{+}$ differentiated cluster 2, that expressed higher levels of mature duct cell markers, such as LCN2 and WFDC2 (Figure S4O) (Bergen et al., 2020). In conclusion, using single-cell sequencing, we found that organoids represent the ductal basal cell compartment when cultured in EM. Exposure to DM induced broad transcriptional changes with increased expression of a wide range of tear products.

Lacrimal gland organoids as a model for tearing

The main function of the lacrimal gland is to produce the aqueous layer of the tear film. *In vivo*, neurotransmitters (acetylcholine, vasoactive intestinal peptide [VIP], and noradrenaline) released from stimulated parasympathetic and sympathetic nerves act on ductal cells, acinar cells, and myoepithelium to induce tearing. This phenomenon requires the expression by lacrimal gland cells both of receptors for neurotransmitters and of ion channels (Dartt, 2009). To address if our organoids could respond to neural stimuli, we first examined the expression of receptors for neurotransmitters in our single-cell datasets. We found that the adrenergic receptor *ADRB1*, but not *ADRA1A*, was upregulated in differentiated organoids, although both were lowly expressed in lacrimal gland tissue cells (Figure S4P). The muscarinic receptor *CHRM1* was not expressed by organoid cells in either expansion or differentiation (Figure S4Q). In the tissue, *CHRM1* was more broadly expressed by acinar cells than by ductal cells (Figure S4Q). On the other hand, *CHRM3* was upregulated in differentiated organoids compared to undifferentiated organoids and broadly expressed in primary tissue cells (Figures S4Q and 3G). Finally, *VIPR1*, but not *VIPR2*, was expressed by tissue ductal and acinar cells and upregulated upon differentiation in organoids (Figure S4R). Next, we checked the expression of some known ion channels in organoids and tissue cells. Water secretion follows an electrochemical gradient and therefore requires ion channel expression and opening (Dartt, 2009; Ubels et al., 2006). The chloride channels *CFTR*, *CLCN3*, and *SLC12A4* were largely expressed by organoid cells in both expansion and differentiation, at least as much as in tissue ductal cells (Figure S4S). Lastly, the potassium channel *LRRC26*, which was broadly expressed in tissue cells, was upregulated upon differentiation in the organoids (Figure S4S). This indicated that our lacrimal gland organoid model could be used as a functional model for fluid secretion and therefore tearing.

Hence, we set out to induce tearing in the lacrimal gland organoids. Luminal accumulation of fluids, following an electrochemical gradient, results in the swelling of organoids. Organoid swelling has previously been applied to monitor CFTR function in intestinal tract organoids of patients with cystic fibrosis (Dekkers et al., 2013; Geurts et al., 2020). Using lacrimal gland organoid swelling as a proxy for water secretion by the lacrimal gland, we tested this functional platform to monitor chemical inducers of crying. We exposed differentiated organoids to the following compounds: cAMP/PKA activators FSK and dibutyryl cAMP (dbcAMP), neurotransmitter norepinephrine (NorEpi), the muscarinic receptor activators carbachol and pilocarpine, and VIP (Figure 5A). FSK and dbcAMP were potent activators of secretion, as evidenced by the 50% increase of organoid diameter over a 4-h time period (Figures 5B and 5C). While carbachol did not induce organoid swelling, muscarinic activation mediated by pilocarpine triggered organoid swelling up to 25% of their initial diameter (Figures 5B and 5C). Lastly, adrenergic stimulation by norepinephrine and VIP stimulation both induced organoid swelling up to 50% of their original diameter (Figures 5B and 5C). These data indicate that water secretion occurs upon neurotransmitter exposure in lacrimal gland organoids and suggest that lacrimal gland organoids could be used as a screening platform for tearing inducers (Figure 5D).

Orthotopic transplantation of human lacrimal gland organoids in mouse

To investigate whether human lacrimal gland organoids are able to engraft in lacrimal gland tissue, we orthotopically transplanted organoid cells into lacrimal glands of immunodeficient non-obese diabetic (NOD) severe combined immunodeficiency (SCID) gamma (NSG) mice. To improve cell viability *in vivo*, we transplanted small organoids that were split in EM 3 days before the procedure. We then collected lacrimal glands 2 weeks, 1 month, and 2 months after transplantation (Figure 5E). By screening for the expression of a human nucleolar marker, we found that human organoid cells had formed duct-like structures from 2 weeks onward after transplantation, which remained in the lacrimal gland for at least 2 months (Figure 5F). Engrafted organoids additionally seemed to self-organize, as cell debris were located in the lumen of the duct-like structures, and we identified some rare proliferating cells up to 2 months post-transplant as indicated by KI67 staining (Figures 5G, S5A, and S5D). Engrafted

Please cite this article in press as: Bannier-Hélaouët et al., Exploring the human lacrimal gland using organoids and single-cell sequencing, Cell Stem Cell (2021), https://doi.org/10.1016/j.stem.2021.02.024

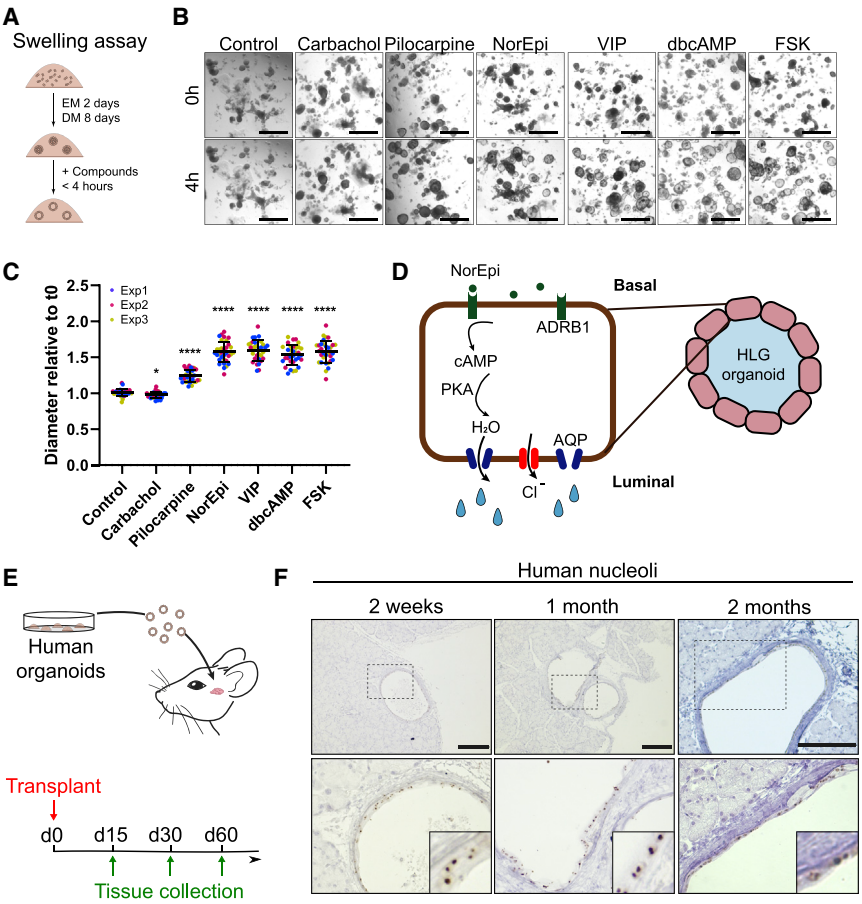

Figure 5. Applications of human lacrimal gland organoids

(A) Schematic representation of organoid swelling assay protocol. After splitting, organoids were cultured in EM for 2 days before being exposed to DM for 8 days. On the experiment day, compounds were added to the organoids, and the swelling was imaged after 4 h.

(B) Swelling assay of human organoids exposed to the following chemical stimuli: 50 mM carbachol, 1 mM dbcAMP, 1 μM FSK, 100 μM norepinephrine (NorEpi), 5 mM pilocarpine, and 250 nM VIP. Scale bars, 1 mm.

(C) Quantification of the swelling as the ratio of organoid diameter 4 h after exposure relative to organoid diameter at 0 h (t0). For each experiment indicated by a color, 11 organoids were measured, and Student's t tests were performed. *$p < 0.05$; ****$p < 0.0001$. Error bars represent SEM.

(D) Schematic representation of organoid "tearing" in response to norepinephrine.

(E) Schematic of the workflow and the timeline of human lacrimal gland organoids transplantation into mouse lacrimal gland.

(F) Representative images of human nucleolar marker staining of human lacrimal gland organoid engraftment 2 weeks, 1 month, and 2 months after organoid injection into mouse lacrimal gland. Scale bars, 200 μm.

(G) Representative stainings for KI67, PAX6, KRT5, and LCN2 of engrafted cells 1 month after transplantation. Scale bars, 50 μm.

See also Figure S5.

cells retained expression of PAX6, LCN2, and KRT5 (Figures 5G and S5A). Similar to the host tissue, human KRT5$^+$ cells were located basally in the duct (Figures 5G and S5A). We also identified LTF$^+$ and LYZ$^+$ cells, suggesting the engrafted organoids have the ability to mature *in vivo* and produce functional tear products, as seen upon exposure to DM *in vitro* (Figure S5B). Detection of tear proteins inside the ducts indicated luminal secretion (Figures 5G, S5A, and S5B). Finally, engrafted organoids were surrounded by a ring of collagen containing Acta2$^+$ cells of mouse origin, similar to mouse lacrimal gland ducts (Figures S5A and S5C). Altogether, this indicated that human lacrimal gland organoids can engraft *in vivo* and retain the expression of mature tear products.

DISCUSSION

Lacrimal glands produce most of the aqueous phase of the tears. As such, they are crucial for maintaining the ocular surface homeostasis. Yet, the cellular heterogeneity and origin of tear components of the lacrimal gland are poorly understood. The ability to culture mature human lacrimal gland epithelium is key to a better understanding of tear gland pathologies and exploring the possibilities of transplanting healthy cells in regenerative therapies.

Here, we describe an adult stem cell-based organoid protocol for long-term expansion of mouse and human ductal cells of the lacrimal gland. Organoids morphologically, transcriptionally, and functionally recapitulate the lacrimal gland ductal epithelium. A detailed look at our EM reveals key signaling pathways in the activation of lacrimal gland adult stem cells. FGF10 was required to establish both murine and human organoids, in line with a murine study (Xiao and Zhang, 2020). Indeed, mesenchymal Fgf10 is an essential growth factor in murine lacrimal gland development and mutations in *FGF10*, *FGFR2*, and *FGFR3* have been described to block correct human lacrimal gland development (Makarenkova et al., 2000; Adams and Schaaf, 2018). The addition of R-spondin and a BMP inhibitor promotes the growth of lacrimal gland organoids, as for many other epithelial organoid models. Transcriptome analysis of murine organoids further highlights the importance of Wnt signaling, with genes such as the well-established Wnt targets *Axin2* and *Lgr5* being upregulated in expansion conditions. *In vivo*, Wnt and BMP signaling

Please cite this article in press as: Bannier-Hélaouët et al., Exploring the human lacrimal gland using organoids and single-cell sequencing, Cell Stem Cell (2021), https://doi.org/10.1016/j.stem.2021.02.024

pathways have been shown to regulate branching morphogenesis during lacrimal gland development (Dean et al., 2005; Liu and Lin, 2014). On the other hand, the human lacrimal gland organoid DM composition was minimal as it only contained N-acetylcysteine and DAPT, a Notch inhibitor. While Notch inhibition has been previously implicated in branching morphogenesis during lacrimal gland development, its role in adulthood remains undetermined (Dvoriantchikova et al., 2017). In our model, Notch inhibition was crucial, as it led to a decrease in proliferation along with an increase in the expression of tear components and mature lacrimal gland markers (such as *CHRM3* and *AQP5*). Taken together, our data suggest that FGF, WNT, BMP, and Notch signaling pathways are important during postnatal lacrimal duct homeostasis.

Pax6 is considered a competence factor for lacrimal gland development, as its loss results in the absence of lacrimal glands (Makarenkova et al., 2000), while induced expression of Pax6 is required for differentiating human pluripotent stem cells into lacrimal gland cells (Hirayama et al., 2017). The role of Pax6 in adult lacrimal gland maintenance has remained unexplored. Using CRISPR-Cas9-mediated genome editing, we show that Pax6 is crucial for the differentiation capacity of murine organoids, without affecting their expansion potential *in vitro*. In particular, Pax6-KO organoids lose the expression of receptors for neurotransmitters, genes involved in the secretion machinery (such as *Aqp5*), tear products, and retinol metabolism-related genes. All of these features are altered in patients with Sjögren's syndrome; patients can harbor autoantibodies against CHRM3 (Cha et al., 2006), display mislocalized AQP5 (Tsubota et al., 2001), and can have altered tear profiles (Brito-Zerón et al., 2016), and retinol treatment can be beneficial to the quality of the tear film (Odaka et al., 2012; Alanazi et al., 2019). In humans, loss of PAX6 in conjunctival tissue has been observed in Sjögren's syndrome patients (McNamara et al., 2014). Alterations in PAX6 expression levels in the lacrimal glands of patients with dry eye disease remain to be investigated. If so, Pax6-KO organoids may provide valuable insights to understand changes in tear secretion observed in dry eye diseases and Sjögren's syndrome (Messmer, 2015; Brito-Zerón et al., 2016). Nevertheless, these data show that Pax6 is essential to maintain adult lacrimal gland duct function and identity.

Single-cell mRNA sequencing is a powerful tool to investigate cellular heterogeneity within tissues (Regev et al., 2017). We applied this technology to human lacrimal gland tissue and organoids. We thus identify tear components, such as *WFDC2*, *PRR27*, *SMR3A*, and *SMR3B*. Some of these have previously been found in human saliva, but not in tears (St Laurent et al., 2015). Second, we describe the heterogeneity of acinar cell populations in the lacrimal gland. We find that beyond the expression of *LYZ*, *LTF*, and *LCN1*, acinar cells produce a large variety of tear components. Acinar cells are transcriptionally different from ductal cells, which produce, for instance, the majority of *LCN2*, *C3*, and *WFDC2* in our cell atlas of the human tear gland.

We find that our lacrimal gland organoid protocol predominantly enables the expansion of ductal progenitors, as also seen in the pancreas and salivary gland organoid cultures (Boj et al., 2015; Maimets et al., 2016), that can then differentiate into tear-producing cells. These observations were corroborated by our single-cell RNA velocity analysis of the organoid dataset. This analysis illustrated that most organoid cells likely originate from *KRT5*$^{+}$ cells, which have been described to be ductal progenitors in mouse (Farmer et al., 2017). We also identified some rare acinar cells expressing *BPIFA1* among our organoid cells.

Treatment options for patients with lacrimal gland disorders are limited partly due to a lack of biological understanding. Patient-derived organoids open up new avenues to study lacrimal gland biology and diseases. The latter can even be done in a personalized fashion by following a similar biobanking approach we have used in the fields of oncology (van de Wetering et al., 2015) and cystic fibrosis (Geurts et al., 2020) or targeting relevant genes utilizing genome editing tools (Drost et al., 2015).

We show that lacrimal gland organoids express a wide range of tear components and can be induced to "cry" upon exposure to pilocarpine, norepinephrine, and VIP. Both carbachol and pilocarpine stimulate tear fluid secretion *in vivo*, but pilocarpine was the only one to induce organoid swelling *in vitro* (Vivino et al., 1999; Fonseca et al., 2015). It has previously been shown in a salivary gland cell line that carbachol and pilocarpine act through different mechanisms, with carbachol acting through M1 and M3 muscarinic receptors and pilocarpine only triggering M3 receptors (Lin et al., 2008). One explanation for our observation may be that carbachol mostly acts on acinar cells through muscarinic receptor 1 (*CHRM1*), which was absent in organoid cells and lowly expressed in tissue ductal cells. This could indicate that *in vivo*, carbachol activates secretion by acinar cells, while pilocarpine promotes secretion by both acinar and ductal cells. Yet, the molecular mechanism for fluid secretion by lacrimal gland duct cells merits further investigations (Katona et al., 2014). Nevertheless, lacrimal gland organoids can be used as a screening platform for compounds that induce tearing mediated by ductal cells and to study secretion mechanisms.

Lastly, given that Sjögren's syndrome is a poorly understood autoimmune disease, co-cultures of lacrimal gland organoids with resident immune cells or autoantibodies could be explored, as previously illustrated with tumor-derived organoids (Dijkstra et al., 2018). Organoid engraftment capacity upon orthotopic transplantation may be used for restoration of lacrimal gland function in patients with dry eye disease, either by transplantation of healthy donor tissue or autologous transplantation upon gene correction *in vitro*. For this, additional validation of the beneficial effects of organoid transplantation in mouse models of dry eye disease is required. In conclusion, organoids represent a tractable model to better understand the biology of the lacrimal gland and study the pathologies of tearing.

Limitations of study

The lacrimal gland contains two main cell types that produce tears: ductal cells and acinar cells. As several other organoid models, our lacrimal gland organoids predominantly represent the ductal compartment of the tissue. This is important to keep in mind with the use of this experimental platform. Additional optimization of lacrimal gland organoid establishment is required to develop acinar cell-derived organoids. Achieving this could also provide a better understanding of acinar cell regeneration.

In addition, we show that lacrimal gland organoids engraft upon orthotopic transplantation. This is an important first step

Please cite this article in press as: Bannier-Hélaouët et al., Exploring the human lacrimal gland using organoids and single-cell sequencing, Cell Stem Cell (2021), https://doi.org/10.1016/j.stem.2021.02.024

for potential regenerative therapies. However, we did not show that organoid engraftment could restore lacrimal gland function. This aspect should be assessed in mouse models of dry eye disease, for instance, before any human application can be envisioned.

STAR★METHODS

Detailed methods are provided in the online version of this paper and include the following:

- KEY RESOURCES TABLE
- RESOURCE AVAILABILITY
  - Lead contact
  - Materials availability
  - Data and code availability
- EXPERIMENTAL MODEL AND SUBJECT DETAILS
  - Patient samples
  - Mice
- METHOD DETAILS
  - Lacrimal gland organoid cultures, reagents
  - Functional swelling assay
  - CRISPR/Cas9-mediated Pax6 knockout
  - Western blot
  - Immunohistochemistry and imaging
  - qPCR analysis
  - Bulk mRNA sequencing
  - Single-cell mRNA sequencing
  - Bioinformatics analysis
  - Organoid transplantation
  - Statistical analysis

SUPPLEMENTAL INFORMATION

Supplemental information can be found online at https://doi.org/10.1016/j.stem.2021.02.024.

ACKNOWLEDGMENTS

We thank Stefan van der Elst, Reinier van der Linden, Rosemary Millen, and Cayetano Pleguezuelos-Manzano for flow cytometry assistance; Anko de Graaff and the Hubrecht Imaging Centre (HIC) for microscopy assistance; Single Cell Discoveries for the provided single-cell sequencing service and support; Utrecht Sequencing (USEQ) for bulk RNA-sequencing services; Gijs van Son for help with bulk RNA-sequencing data mapping; and Adriana Martínez-Silgado for help with Illustrator. Y.P. was supported by a grant from the Leducq Foundation (14CVD03); M.B.-H. was supported by a NWO-ZonW grant (114021013); H.G., Y.E.B.E., and H.C. were supported by an ERC Advanced Grant (agreement 67013e); H.G. was supported by a VENI grant from NWO-ZonMW (016.166.119); and J.v.d.V. was supported by the gravitation program CancerGenomiCs.nl from the Netherlands Organisation for Scientific Research (NWO).

AUTHOR CONTRIBUTIONS

M.B.-H., Y.P., and H.C. conceived and designed the project. M.B.-H., Y.P., and M.T.B. performed experiments. M.B.-H. performed analysis of RNA-sequencing data with help from H.G. *In vivo* transplantation was done by J.K. Y.E.B.-E. assisted with fluorescence-activated cell sorting (FACS) for single-cell sequencing. J.v.d.V. helped generate RNA-sequencing data. M.B.-H., H.B., and J.K. generated IHC data. R.K. and S.M.I. provided access to human tissue. M.B.-H., Y.P., and H.C. wrote the manuscript, with input from all authors.

DECLARATION OF INTERESTS

H.C. is the inventor on several patents related to organoid technology; his full disclosure is given at https://www.uu.nl/staff/JCClevers/. Y.P. is an employee of Surrozen and was an employee of the Hubrecht Institute when this work was performed and completed.

Received: May 9, 2020
Revised: January 11, 2021
Accepted: February 18, 2021
Published: March 16, 2021

REFERENCES

Adams, J., and Schaaf, C.P. (2018). Diagnosis and genetics of alacrima. Clin. Genet. *94*, 54–60.

Alanazi, S.A., El-Hiti, G.A., Al-Baloud, A.A., Alfarhan, M.I., Al-Shahrani, A., Albakri, A.A., Alqahtani, S., and Masmali, A.M. (2019). Effects of short-term oral vitamin A supplementation on the ocular tear film in patients with dry eye. Clin. Ophthalmol. *13*, 599–604.

Bergen, V., Lange, M., Peidli, S., Wolf, F.A., and Theis, F.J. (2020). Generalizing RNA velocity to transient cell states through dynamical modeling. Nat. Biotechnol. *38*, 1408–1414.

Boj, S.F., Hwang, C.-I., Baker, L.A., Chio, I.I.C., Engle, D.D., Corbo, V., Jager, M., Ponz-Sarvise, M., Tiriac, H., Spector, M.S., et al. (2015). Organoid models of human and mouse ductal pancreatic cancer. Cell *160*, 324–338.

Brito-Zerón, P., Baldini, C., Bootsma, H., Bowman, S.J., Jonsson, R., Mariette, X., Sivils, K., Theander, E., Tzioufas, A., and Ramos-Casals, M. (2016). Sjögren syndrome. Nat. Rev. Dis. Primers *2*, 16047.

Cha, S., Singson, E., Cornelius, J., Yagna, J.P., Knot, H.J., and Peck, A.B. (2006). Muscarinic acetylcholine type-3 receptor desensitization due to chronic exposure to Sjögren's syndrome-associated autoantibodies. J. Rheumatol. *33*, 296–306.

Chow, R.L., Altmann, C.R., Lang, R.A., and Hemmati-Brivanlou, A. (1999). Pax6 induces ectopic eyes in a vertebrate. Development *126*, 4213–4222.

Clevers, H. (2016). Modeling Development and Disease with Organoids. Cell *165*, 1586–1597.

Dartt, D.A. (2009). Neural regulation of lacrimal gland secretory processes: relevance in dry eye diseases. Prog. Retin. Eye Res. *28*, 155–177.

Dean, C.H., Miller, L.-A.D., Smith, A.N., Dufort, D., Lang, R.A., and Niswander, L.A. (2005). Canonical Wnt signaling negatively regulates branching morphogenesis of the lung and lacrimal gland. Dev. Biol. *286*, 270–286.

Dekkers, J.F., Wiegerinck, C.L., de Jonge, H.R., Bronsveld, I., Janssens, H.M., de Winter-de Groot, K.M., Brandsma, A.M., de Jong, N.W.M., Bijvelds, M.J.C., Scholte, B.J., et al. (2013). A functional CFTR assay using primary cystic fibrosis intestinal organoids. Nat. Med. *19*, 939–945.

Dijkstra, K.K., Cattaneo, C.M., Weeber, F., Chalabi, M., van de Haar, J., Fanchi, L.F., Slagter, M., van der Velden, D.L., Kaing, S., Kelderman, S., et al. (2018). Generation of Tumor-Reactive T Cells by Co-culture of Peripheral Blood Lymphocytes and Tumor Organoids. Cell *174*, 1586–1598.e12.

Dor, M., Eperon, S., Lalive, P.H., Guex-Crosier, Y., Hamedani, M., Salvisberg, C., and Turck, N. (2019). Investigation of the global protein content from healthy human tears. Exp. Eye Res. *179*, 64–74.

Drost, J., van Jaarsveld, R.H., Ponsioen, B., Zimberlin, C., van Boxtel, R., Buijs, A., Sachs, N., Overmeer, R.M., Offerhaus, G.J., Begthel, H., et al. (2015). Sequential cancer mutations in cultured human intestinal stem cells. Nature *521*, 43–47.

Drost, J., Karthaus, W.R., Gao, D., Driehuis, E., Sawyers, C.L., Chen, Y., and Clevers, H. (2016). Organoid culture systems for prostate epithelial and cancer tissue. Nat. Protoc. *11*, 347–358.

Dvoriantchikova, G., Tao, W., Pappas, S., Gaidosh, G., Tse, D.T., Ivanov, D., and Pelaez, D. (2017). Molecular Profiling of the Developing Lacrimal Gland Reveals Putative Role of Notch Signaling in Branching Morphogenesis. Invest. Ophthalmol. Vis. Sci. *58*, 1098–1109.

Please cite this article in press as: Bannier-Hélaouët et al., Exploring the human lacrimal gland using organoids and single-cell sequencing, Cell Stem Cell (2021), https://doi.org/10.1016/j.stem.2021.02.024

Farmer, D.T., Nathan, S., Finley, J.K., Shengyang Yu, K., Emmerson, E., Byrnes, L.E., Sneddon, J.B., McManus, M.T., Tward, A.D., and Knox, S.M. (2017). Defining epithelial cell dynamics and lineage relationships in the developing lacrimal gland. Development *144*, 2517–2528.

Fonseca, B., Martínez-Águila, A., Díaz-Hernández, M., and Pintor, J. (2015). Diadenosine tetraphosphate contributes to carbachol-induced tear secretion. Purinergic Signal. *11*, 87–93.

Fu, X.W., Song, P.F., and Spindel, E.R. (2015). Role of Lynx1 and related Ly6 proteins as modulators of cholinergic signaling in normal and neoplastic bronchial epithelium. Int. Immunopharmacol. *29*, 93–98.

Fujii, A., Morimoto-Tochigi, A., Walkup, R.D., Shearer, T.R., and Azuma, M. (2013). Lacritin-induced secretion of tear proteins from cultured monkey lacrimal acinar cells. Invest. Ophthalmol. Vis. Sci. *54*, 2533–2540.

Fujii, M., Matano, M., Nanki, K., and Sato, T. (2015). Efficient genetic engineering of human intestinal organoids using electroporation. Nat. Protoc. *10*, 1474–1485.

Geurts, M.H., de Poel, E., Amatngalim, G.D., Oka, R., Meijers, F.M., Kruisselbrink, E., van Mourik, P., Berkers, G., de Winter-de Groot, K.M., Michel, S., et al. (2020). CRISPR-Based Adenine Editors Correct Nonsense Mutations in a Cystic Fibrosis Organoid Biobank. Cell Stem Cell *26*, 503–510.e7.

Grün, D., Lyubimova, A., Kester, L., Wiebrands, K., Basak, O., Sasaki, N., Clevers, H., and van Oudenaarden, A. (2015). Single-cell messenger RNA sequencing reveals rare intestinal cell types. Nature *525*, 251–255.

Halder, G., Callaerts, P., and Gehring, W.J. (1995). Induction of ectopic eyes by targeted expression of the eyeless gene in Drosophila. Science *267*, 1788–1792.

Hashimshony, T., Senderovich, N., Avital, G., Klochendler, A., de Leeuw, Y., Anavy, L., Gennert, D., Li, S., Livak, K.J., Rozenblatt-Rosen, O., et al. (2016). CEL-Seq2: sensitive highly-multiplexed single-cell RNA-Seq. Genome Biol *17*.

Hay, D.I., Bennick, A., Schlesinger, D.H., Minaguchi, K., Madapallimattam, G., and Schluckebier, S.K. (1988). The primary structures of six human salivary acidic proline-rich proteins (PRP-1, PRP-2, PRP-3, PRP-4, PIF-s and PIF-f). Biochem. J. *255*, 15–21.

Herman, J.S., Sagar, and Grün, D. (2018). FateID infers cell fate bias in multipotent progenitors from single-cell RNA-seq data. Nat. Methods *15*, 379–386.

Hirayama, M., Ogawa, M., Oshima, M., Sekine, Y., Ishida, K., Yamashita, K., Ikeda, K., Shimmura, S., Kawakita, T., Tsubota, K., and Tsuji, T. (2013). Functional lacrimal gland regeneration by transplantation of a bioengineered organ germ. Nat. Commun. *4*, 2497.

Hirayama, M., Ko, S.B.H., Kawakita, T., Akiyama, T., Goparaju, S.K., Soma, A., Nakatake, Y., Sakota, M., Chikazawa-Nohtomi, N., Shimmura, S., et al. (2017). Identification of transcription factors that promote the differentiation of human pluripotent stem cells into lacrimal gland epithelium-like cells. NPJ Aging Mech. Dis. *3*, 1.

Hodges, R.R., and Dartt, D.A. (2003). Regulatory pathways in lacrimal gland epithelium. Int. Rev. Cytol. *231*, 129–196.

Hodges, R.R., and Dartt, D.A. (2016). Signaling Pathways of Purinergic Receptors and Their Interactions with Cholinergic and Adrenergic Pathways in the Lacrimal Gland. J. Ocul. Pharmacol. Ther. *32*, 490–497.

Hu, H., Gehart, H., Artegiani, B., LÖpez-Iglesias, C., Dekkers, F., Basak, O., van Es, J., Chuva de Sousa Lopes, S.M., Begthel, H., Korving, J., et al. (2018). Long-Term Expansion of Functional Mouse and Human Hepatocytes as 3D Organoids. Cell *175*, 1591–1606.e19.

Hua, L., Liu, Y., Zhen, S., Wan, D., Cao, J., and Gao, X. (2014). Expression and biochemical characterization of recombinant human epididymis protein 4. Protein Expr. Purif. *102*, 52–62.

Jenssen, H., and Hancock, R.E.W. (2009). Antimicrobial properties of lactoferrin. Biochimie *91*, 19–29.

Kalmodia, S., Son, K.-N., Cao, D., Lee, B.-S., Surenkhuu, B., Shah, D., Ali, M., Balasubramaniam, A., Jain, S., and Aakalu, V.K. (2019). Presence of Histatin-1 in Human Tears and Association with Aqueous Deficient Dry Eye Diagnosis: A Preliminary Study. Sci. Rep. *9*, 10304.

Katona, M., Vizvári, E., Németh, L., Facskó, A., Venglovecz, V., Rakonczay, Z., Jr., Hegyi, P., and Tóth-Molnár, E. (2014). Experimental evidence of fluid secretion of rabbit lacrimal gland duct epithelium. Invest. Ophthalmol. Vis. Sci. *55*, 4360–4367.

Lehrer, R.I., Xu, G., Abduragimov, A., Dinh, N.N., Qu, X.D., Martin, D., and Glasgow, B.J. (1998). Lipophilin, a novel heterodimeric protein of human tears. FEBS Lett. *432*, 163–167.

Lin, A.L., Zhu, B., Zhang, W., Dang, H., Zhang, B.-X., Katz, M.S., and Yeh, C.-K. (2008). Distinct pathways of ERK activation by the muscarinic agonists pilocarpine and carbachol in a human salivary cell line. Am. J. Physiol. Cell Physiol. *294*, C1454–C1464.

Lin, H., Liu, Y., and Yiu, S. (2019). Three Dimensional Culture of Potential Epithelial Progenitor Cells in Human Lacrimal Gland. Transl. Vis. Sci. Technol. *8*, 32.

Liu, Y., and Lin, D. (2014). Necessity of Smad4 for the normal development of the mouse lacrimal gland. Jpn. J. Ophthalmol. *58*, 298–306.

Love, M.I., Huber, W., and Anders, S. (2014). Moderated estimation of fold change and dispersion for RNA-seq data with DESeq2. Genome Biol. *15*, 550.

Maimets, M., Rocchi, C., Bron, R., Pringle, S., Kuipers, J., Giepmans, B.N.G., Vries, R.G.J., Clevers, H., de Haan, G., van Os, R., and Coppes, R.P. (2016). Long-Term In Vitro Expansion of Salivary Gland Stem Cells Driven by Wnt Signals. Stem Cell Reports *6*, 150–162.

Makarenkova, H.P., and Dartt, D.A. (2015). Myoepithelial Cells: Their Origin and Function in Lacrimal Gland Morphogenesis, Homeostasis, and Repair. Curr. Mol. Biol. Rep. *1*, 115–123.

Makarenkova, H.P., Ito, M., Govindarajan, V., Faber, S.C., Sun, L., McMahon, G., Overbeek, P.A., and Lang, R.A. (2000). FGF10 is an inducer and Pax6 a competence factor for lacrimal gland development. Development *127*, 2563–2572.

Massie, I., Spaniol, K., Barbian, A., Geerling, G., Metzger, M., and Schrader, S. (2018). Development of lacrimal gland spheroids for lacrimal gland tissue regeneration. J. Tissue Eng. Regen. Med. *12*, e2001–e2009.

McKown, R.L., Coleman Frazier, E.V., Zadrozny, K.K., Deleault, A.M., Raab, R.W., Ryan, D.S., Sia, R.K., Lee, J.K., and Laurie, G.W. (2014). A cleavage-potentiated fragment of tear lacritin is bactericidal. J. Biol. Chem. *289*, 22172–22182.

McNamara, N.A., Gallup, M., and Porco, T.C. (2014). Establishing PAX6 as a biomarker to detect early loss of ocular phenotype in human patients with Sjögren's syndrome. Invest. Ophthalmol. Vis. Sci. *55*, 7079–7084.

Messmer, E.M. (2015). The pathophysiology, diagnosis, and treatment of dry eye disease. Dtsch. Arzteblatt Int *112*, 71–81, quiz 82.

Muraro, M.J., Dharmadhikari, G., Grün, D., Groen, N., Dielen, T., Jansen, E., van Gurp, L., Engelse, M.A., Carlotti, F., de Koning, E.J.P., and van Oudenaarden, A. (2016). A Single-Cell Transcriptome Atlas of the Human Pancreas. Cell Syst. *3*, 385–394.e3.

Navone, R., Lunardi, C., Gerli, R., Tinazzi, E., Peterlana, D., Bason, C., Corrocher, R., and Puccetti, A. (2005). Identification of tear lipocalin as a novel autoantigen target in Sjögren's syndrome. J. Autoimmun. *25*, 229–234.

Odaka, A., Toshida, H., Ohta, T., Tabuchi, N., Koike, D., Suto, C., and Murakami, A. (2012). Efficacy of retinol palmitate eye drops for dry eye in rabbits with lacrimal gland resection. Clin. Ophthalmol. *6*, 1585–1593.

Perumal, N., Funke, S., Pfeiffer, N., and Grus, F.H. (2016). Proteomics analysis of human tears from aqueous-deficient and evaporative dry eye patients. Sci. Rep. *6*, 29629.

Ran, F.A., Hsu, P.D., Wright, J., Agarwala, V., Scott, D.A., and Zhang, F. (2013). Genome engineering using the CRISPR-Cas9 system. Nat. Protoc. *8*, 2281–2308.

Regev, A., Teichmann, S.A., Lander, E.S., Amit, I., Benoist, C., Birney, E., Bodenmiller, B., Campbell, P., Carninci, P., Clatworthy, M., et al.; Human Cell Atlas Meeting Participants (2017). The Human Cell Atlas. eLife *6*, e27041.

Samarawickrama, C., Chew, S., and Watson, S. (2015). Retinoic acid and the ocular surface. Surv. Ophthalmol. *60*, 183–195.

Sato, T., Vries, R.G., Snippert, H.J., van de Wetering, M., Barker, N., Stange, D.E., van Es, J.H., Abo, A., Kujala, P., Peters, P.J., and Clevers, H. (2009).

Please cite this article in press as: Bannier-Hélaouët et al., Exploring the human lacrimal gland using organoids and single-cell sequencing, Cell Stem Cell (2021), https://doi.org/10.1016/j.stem.2021.02.024

Single Lgr5 stem cells build crypt-villus structures in vitro without a mesenchymal niche. Nature *459*, 262–265.

Sato, T., Stange, D.E., Ferrante, M., Vries, R.G.J., Van Es, J.H., Van den Brink, S., Van Houdt, W.J., Pronk, A., Van Gorp, J., Siersema, P.D., and Clevers, H. (2011). Long-term expansion of epithelial organoids from human colon, adenoma, adenocarcinoma, and Barrett's epithelium. Gastroenterology *141*, 1762–1772.

Schlesinger, D.H., Hay, D.I., Schluckebier, S.K., and Ahern, J.M. (1994). Primary structure of a novel human salivary acidic proline-rich protein. Pept. Res. *7*, 242–247.

Schutgens, F., Rookmaaker, M.B., Margaritis, T., Rios, A., Ammerlaan, C., Jansen, J., Gijzen, L., Vormann, M., Vonk, A., Viveen, M., et al. (2019). Tubuloids derived from human adult kidney and urine for personalized disease modeling. Nat. Biotechnol. *37*, 303–313.

St Laurent, C.D., St Laurent, K.E., Mathison, R.D., and Befus, A.D. (2015). Calcium-binding protein, spermatid-specific 1 is expressed in human salivary glands and contains an anti-inflammatory motif. Am. J. Physiol. Regul. Integr. Comp. Physiol. *308*, R569–R575.

Stange, D.E., Koo, B.-K., Huch, M., Sibbel, G., Basak, O., Lyubimova, A., Kujala, P., Bartfeld, S., Koster, J., Geahlen, J.H., et al. (2013). Differentiated Troy+ chief cells act as reserve stem cells to generate all lineages of the stomach epithelium. Cell *155*, 357–368.

Tiwari, S., Ali, M.J., Balla, M.M.S., Naik, M.N., Honavar, S.G., Reddy, V.A.P., and Vemuganti, G.K. (2012). Establishing human lacrimal gland cultures with secretory function. PLoS ONE *7*, e29458.

Torres, P., Castro, M., Reyes, M., and Torres, V.A. (2018). Histatins, wound healing, and cell migration. Oral Dis. *24*, 1150–1160.

Tsou, Y.-A., Tung, M.-C., Alexander, K.A., Chang, W.-D., Tsai, M.-H., Chen, H.-L., and Chen, C.-M. (2018). The Role of BPIFA1 in Upper Airway Microbial Infections and Correlated Diseases. BioMed Res. Int. *2018*, 2021890.

Tsubota, K., Hirai, S., King, L.S., Agre, P., and Ishida, N. (2001). Defective cellular trafficking of lacrimal gland aquaporin-5 in Sjögren's syndrome. Lancet *357*, 688–689.

Turner, H.C., Budak, M.T., Akinci, M.A., and Wolosin, J.M. (2007). Comparative analysis of human conjunctival and corneal epithelial gene expression with oligonucleotide microarrays. Invest. Ophthalmol. Vis. Sci. *48*, 2050–2061.

Ubels, J.L., Hoffman, H.M., Srikanth, S., Resau, J.H., and Webb, C.P. (2006). Gene expression in rat lacrimal gland duct cells collected using laser capture microdissection: evidence for K+ secretion by duct cells. Invest. Ophthalmol. Vis. Sci. *47*, 1876–1885.

van de Wetering, M., Francies, H.E., Francis, J.M., Bounova, G., Iorio, F., Pronk, A., van Houdt, W., van Gorp, J., Taylor-Weiner, A., Kester, L., et al. (2015). Prospective derivation of a living organoid biobank of colorectal cancer patients. Cell *161*, 933–945.

Vieira, F., Kung, J.W., and Bhatti, F. (2017). Structure, genetics and function of the pulmonary associated surfactant proteins A and D: The extra-pulmonary role of these C type lectins. Ann. Anat. *211*, 184–201.

Vivino, F.B., Al-Hashimi, I., Khan, Z., LeVeque, F.G., Salisbury, P.L., 3rd, Tran-Johnson, T.K., Muscoplat, C.C., Trivedi, M., Goldlust, B., and Gallagher, S.C. (1999). Pilocarpine tablets for the treatment of dry mouth and dry eye symptoms in patients with Sjögren syndrome: a randomized, placebo-controlled, fixed-dose, multicenter trial. P92-01 Study Group. Arch. Intern. Med. *159*, 174–181.

Willcox, M.D., Morris, C.A., Thakur, A., Sack, R.A., Wickson, J., and Boey, W. (1997). Complement and complement regulatory proteins in human tears. Invest. Ophthalmol. Vis. Sci. *38*, 1–8.

Xiao, S., and Zhang, Y. (2020). Establishment of long-term serum-free culture for lacrimal gland stem cells aiming at lacrimal gland repair. Stem Cell Res. Ther. *11*, 20.

Young, M.D., Wakefield, M.J., Smyth, G.K., and Oshlack, A. (2010). Gene ontology analysis for RNA-seq: accounting for selection bias. Genome Biol. *11*, R14.

Please cite this article in press as: Bannier-Hélaouët et al., Exploring the human lacrimal gland using organoids and single-cell sequencing, Cell Stem Cell (2021), https://doi.org/10.1016/j.stem.2021.02.024

CellPress

STAR★METHODS

KEY RESOURCES TABLE

REAGENT or RESOURCE	SOURCE	IDENTIFIER
Antibodies		
Anti-Pax6	Biolegend	90131; RRID: AB_2565003
Anti-Lipocalin 2	R&D Systems	AF1757; RRID: AB_354974
Anti-ZO1	Life Technologies	40-2200; RRID: AB_2533456
Anti-Lactotransferrin	Millipore	07-685; RRID: AB_390172
Anti-Aquaporin 5	Origene	TA321387
Anti-Keratin 5	Covance	905501; RRID: AB_2565050
Anti-Lysozyme	Dako	A0099; RRID: AB_2341230
Anti-ACTA2	Sigma-Aldrich	A5228; RRID: AB_262054
Anti-WFDC2	LSBio	LS-C175346
Anti-PRR27	Thermo Fisher scientific	PA5-57546; RRID: AB_2645996
Anti-Histatin 1	Mybiosource	MBS2002621
Anti-Lipocalin 1	Santa Cruz	sc-374620; RRID: AB_10988774
Anti-BPIFA1	Thermo Fisher scientific	PA5-42187; RRID: AB_2577132
Anti-SCGB2A1	Atlas antibodies	HPA034584; RRID: AB_10602221
Anti-TP63	Abcam	ab735; RRID: AB_305870
Anti-KI67	eBiosciences	14-5698-82; RRID: AB_10854564
Anti-Human nucleoli	Abcam	ab-190710
Anti-Hsp90	Origene	TA500494; RRID: AB_2121397
Alexa Fluor 488 donkey anti-rabbit	Thermo Fisher scientific	A21206; RRID: AB_2535792
Alexa Fluor 568 donkey anti-mouse	Thermo Fisher scientific	A10037; RRID: AB_2534013
Alexa Fluor 568 donkey anti-rabbit	Thermo Fisher scientific	A10042; RRID: AB_2534017
Alexa Fluor 568 donkey anti-goat	Thermo Fisher scientific	A11057; RRID: AB_2534104
Alexa Fluor 555 goat anti-rat	Thermo Fisher scientific	A21434; RRID: AB_2535855
Phalloidin–Atto 647N	Sigma-Aldrich	65906
Rabbit anti-goat IgG(H+L)-UNLB	Southern Biotech	6160-01; RRID: AB_2796227
Rabbit Anti-Rat IgG(H+L), Human ads-UNLB	Southern Biotech	6185-01; RRID: AB_2796259
Swine anti-rabbit HRP	Dako	P021702-2
Rabbit anti-goat HRP	Dako	P044901-2
EnVision+/HRP mouse	Agilent	K400111-2
EnVision+/HRP rabbit	Agilent	K400311-2
Biological samples		
Human lacrimal gland tissue	Utrecht Medical Center	TCbio protocol 18-740
Mouse lacrimal gland tissue for organoids	Hubrecht Institute	N/A
NSG mice	Hubrecht Institute	Project license: AVD8010020151
Chemicals, peptides, and recombinant proteins		
Accutase	Thermo Fisher scientific	00-4555
Dispase	Thermo Fisher scientific	17105-041
Collagenase I	Sigma-Aldrich	C9407
Cell Recovery	Corning	354253
PVDF membrane	Millipore	IPVH00010
Bradford assay	Bio-Rad	500-0006
Complete mini protease inhibitor cocktail tablets	Roche	11836170001

(*Continued on next page*)

Please cite this article in press as: Bannier-Hélaouët et al., Exploring the human lacrimal gland using organoids and single-cell sequencing, Cell Stem Cell (2021), https://doi.org/10.1016/j.stem.2021.02.024

Continued

REAGENT or RESOURCE	SOURCE	IDENTIFIER
CellTiterGlo 3D	Promega	G9683
Advanced DMEM/F12	Thermo Fisher scientific	12634-010
B-27 Supplement	Thermo Fisher scientific	17504044
GlutaMAX	Thermo Fisher scientific	35050061
HEPES	Thermo Fisher scientific	15630080
Penicillin-Streptomycin	Thermo Fisher scientific	15140122
Noggin conditioned medium	U-Protein Express	Custom order
R-spondin 3 conditioned medium	U-Protein Express	Custom order
N-Acetyl-L-cysteine	Sigma-Aldrich	A9165
Nicotinamide	Sigma-Aldrich	N0636
FGF10	Peprotech	100-26
Prostaglandin E2	Tocris	2296
Forskolin	Tocris	1099
A83-01	Tocris	2939
Y-27632 dihydrochloride	Abmole	M1817
DAPT	Sigma-Aldrich	D5942
Primocin	Invivogen	ant-pm-2
Cultrex Basement Membrane Extract (BME), Growth Factor Reduced, Type 2	R&D Systems, Bio-Techne	3533-001-02
dbcAMP	Sigma-Aldrich	D0627
Vasoactive Intestinal Peptide (VIP)	Sigma-Aldrich	V3628
Norepinephrine	Sigma-Aldrich	A7257
Carbachol	Sigma-Aldrich	C4382
Pilocarpine	Sigma-Aldrich	P6503
DAPI	Thermo Fisher scientific	D1306
ProLong Gold Antifade Mountant with DAPI	Thermo Fisher scientific	P36935
Formaldehyde solution 4%	Sigma-Aldrich	1.00496
SYBR Green	Bio-Rad	1725270
BSA	MP biomedicals	160069
Donkey serum	Golden Bridge International	E27-100
Triton X-100	Sigma-Aldrich	X100-100ML
SORT-seq reagents	Muraro et al., 2016	N/A
Hematoxylin	Sigma-Aldrich	1159380025
Eosin	Sigma-Aldrich	E4009
Picro-Sirius Red	Sigma-Aldrich	365548
Pertex	Klinipath	AM-08010
pSpCas9(BB)-2A-GFP gRNA cloning reagents	Ran et al., 2013	N/A
BTXpress solution	BTX	45-0805
Complete mini protease inhibitor cocktail tablets	Roche	11836170001
CellTiterGlo 3D	Promega	G9683
Critical commercial assays		
RNeasy Mini Kit	QIAGEN	74104
QIAquick PCR Purification Kit	QIAGEN	28104
Thermo Scientific reagents for CEL-Seq2	(Hashimshony et al., 2016)	
TruSeq Stranded mRNA kit	Illumina	N/A
Miniprep DNA isolation kit	Thermo Fisher scientific	K210003
Midiprep DNA isolation kit	Thermo Fisher scientific	K210005

(*Continued on next page*)

Please cite this article in press as: Bannier-Hélaouët et al., Exploring the human lacrimal gland using organoids and single-cell sequencing, Cell Stem Cell (2021), https://doi.org/10.1016/j.stem.2021.02.024

Continued

REAGENT or RESOURCE	SOURCE	IDENTIFIER
12% Mini-PROTEAN precast protein gel 10-well 30 μL	Bio-Rad	4561043
ECL Prime western blotting detection reagent	GE Healthcare Life Sciences	RPN2232
Deposited data		
Raw and analyzed mouse bulk mRNA sequencing data	Gene expression omnibus https://www.ncbi.nlm.nih.gov/geo/	GEO: GSE164463
Raw and analyzed human single-cell mRNA sequencing data	Gene expression omnibus https://www.ncbi.nlm.nih.gov/geo/	GEO: GSE164403
Experimental models: organisms/strains		
C57BL/6 mice	Hubrecht Institute	N/A
NOD Scid Gamma (NSG) mice	Hubrecht Institute	N/A
Oligonucleotides		
qPCR primers	This paper, Table S5	N/A
Pax6 sgRNA: CCCGGCAGAAGATCGTAGAG	This paper	N/A
Pax6-KO genotyping Pax6_F1: TCCAGTGGGCAGGTTCAAAT	This paper	N/A
Pax6-KO genotyping Pax6_R1: GGAAGGGCACTCCCGTTTAT	This paper	N/A
Pax6-KO genotyping Pax6_F2: ATCATAGACGCGCTCCTTCC	This paper	N/A
Pax6-KO genotyping Pax6_R2: CACAAGCGTGATGGATGCAA	This paper	N/A
Software and algorithms		
CFX manager software	Bio-Rad	N/A
RaceID3	Herman et al., 2018	https://github.com/dgrun/RaceID3_StemID2
scVelo	Bergen et al., 2020	https://github.com/theislab/scvelo
DESeq2	Love et al., 2014	https://github.com/mikelove/DESeq2
GOseq	Young et al., 2010	https://rdrr.io/github/nadiadavidson/goseq/
Rstudio	Rstudio	https://rstudio.com/
Python	Python	https://www.python.org/
GraphPad PRISM 8	GraphPad	N/A
Las X	Leica	N/A
Adobe illustrator	Adobe inc.	N/A
Fiji	NIH, Fiji developers	https://imagej.net/Fiji
Other		
Human tear proteome data	Table S3 (Dor et al., 2019)	N/A
EVOS FL Auto 2 Cell Imaging System	Thermo Fisher scientific	N/A
ImageQuant LAS 4000 ECL western blot imager	GE Healthcare Life Sciences	N/A
SP8 confocal microscope	Leica	N/A
SP8X confocal microscope	Leica	N/A
DM4000	Leica	N/A
NEPA21 electroporator	Nepagene	N/A
CFX384 Touch Real-Time PCR detection system	Bio-Rad	N/A
Spark multimode microplate reader	Tecan	N/A
FACSFusion	BD Biosciences	N/A

(*Continued on next page*)

Please cite this article in press as: Bannier-Hélaouët et al., Exploring the human lacrimal gland using organoids and single-cell sequencing, Cell Stem Cell (2021), https://doi.org/10.1016/j.stem.2021.02.024

Continued

REAGENT or RESOURCE	SOURCE	IDENTIFIER
FACSAria	BD Biosciences	N/A
FACSJazz	BD Biosciences	N/A
FACSMelody	BD Biosciences	N/A

RESOURCE AVAILABILITY

Lead contact

Further information and requests for resources and reagents should be directed to the lead contact, Hans Clevers (h.clevers@hubrecht.eu).

Materials availability

Unique/stable reagents generated in this study are available and can be requested from the lead contact; a completed Materials Transfer Agreement may be required.

Data and code availability

All bulk and single-cell mRNA sequencing data of this study have been deposited in the Gene Expression Omnibus (GEO) under accession numbers GEO: GSE164463 (mouse bulk mRNA sequencing data) and GEO: GSE164403 (human single-cell mRNA sequencing data).

EXPERIMENTAL MODEL AND SUBJECT DETAILS

Patient samples

Human lacrimal gland biopsies were anonymously obtained from Rachel Kalmann and Saskia M. Imhoff at the University Medical Center Utrecht (UMCU) from waste material of patients undergoing surgery at the UMCU. The use of sample for research was approved by the medical ethical committee (TCBio) of the UMCU as protocol 18-740 and was in accordance with the Declaration of Helsinki and according to Dutch law. This study is compliant with all relevant ethical regulations regarding research involving human participants.

Mice

All animal experiments were performed after institutional review by the Animal Ethics Committee of the Royal Netherlands Academy of Arts and Sciences (KNAW) with project license AVD8010020151. Surplus material from female C57BL/6 was used to derive organoids in this study. Transplantation experiments were approved by the Central Authority for Scientific Procedures on Animals (CCD) and the local animal experimental committee at the Hubrecht Institute (IvD-HI-KNAW HI19.1006). Immunodeficient NOD Scid Gamma (NSG) mice aged 7 weeks were used for transplantation experiments.

METHOD DETAILS

Lacrimal gland organoid cultures, reagents

Human samples were kept in Advanced DMEM/F12 solution (GIBCO) with Pen/Strep (Thermo Fisher scientific) at 4°C until further processing. For both mouse and human, complete or part of the gland was chopped into small pieces of approximately 1 mm using a scalpel. Muscle and connective tissue were removed and discarded as much as possible. Epithelial tissue pieces were enzymatically digested in 5 mL collagenase (Sigma-Aldrich, C9407, 1 mg/mL) with 10 μM ROCK inhibitor Y-27632 (Abmole, M1817) in AdDMEM/F12 (GIBCO) for about 15 minutes shaking (120 RPM) at 37°C. The homogeneous cell suspension was pelleted and washed twice with AdDMEM/F12 prior to plating. Cells from a single murine lacrimal gland were plated in approximately 75 uL Cultrex Pathclear Reduced Growth Factor Basement Membrane Extract (BME) (3533-001, Amsbio). For human biopsies the volume of BME was determined based on the size of the final pellet. After BME solidification, complete expansion medium was added.

Mouse expansion medium consisted in AdDMEM/F12 (GIBCO) supplemented with B27, Glutamax, HEPES, 100 U/mL Penicillin-Streptomycin (all Thermo Fisher scientific), 100 mg/mL Primocin (Invivogen), 1.25 mM N-acetylcysteine, 10 mM nicotinamide (both Sigma-Aldrich) and the following growth factors: 1% Noggin conditioned medium (U-Protein Express), 1% R-spondin 3 conditioned medium (U-Protein Express), 0.5 μM A83-01 (Tocris), 1 μM PGE2 (Tocris), 1 μM FSK (Tocris) and 100 ng/mL FGF10 (Peprotech). To differentiate mouse organoids, 2 days after splitting the organoids in expansion medium, we removed R-spondin 3, Noggin, A83-01, PGE2, Nicotinamide and N-acetylcysteine from the medium for five days.

Human expansion medium contained AdDMEM/F12 (GIBCO) supplemented with B27, Glutamax, HEPES, 100 U/mL Penicillin-Streptomycin (all Thermo Fisher scientific), 100 mg/mL Primocin (Invivogen), 1.25 mM N-acetylcysteine (Sigma-Aldrich) and the following growth factors: 2% Noggin conditioned medium (U-Protein Express), 2% R-spondin 3 conditioned medium (U-Protein Express), 0.5 μM A83-01 (Tocris), 1 μM FSK (Tocris) and 100 ng/mL FGF10 (Peprotech). To differentiate human organoids, we split

Please cite this article in press as: Bannier-Hélaouët et al., Exploring the human lacrimal gland using organoids and single-cell sequencing, Cell Stem Cell (2021), https://doi.org/10.1016/j.stem.2021.02.024

them in expansion medium for 2 days then switch to differentiation medium for 7 days. The differentiation medium that was working best and is presented here consisted in AdDMEM/F12 (GIBCO), Glutamax, HEPES, 100 U/mL Penicillin-Streptomycin (all Thermo Fisher scientific), 1.25 mM N-acetylcysteine (Sigma-Aldrich) and 10 μM DAPT (Sigma).

Ten days after seeding, human and mouse organoids were removed from the BME, mechanically dissociated into small fragments using a narrowed Pasteur pipette and re-seeded in fresh BME. Passage was performed in 1:3 – 1:5 split ratio once every 7 - 10 days for at least 40 weeks for mouse and 6 months for human. After initial seeding (passage 0) or after splitting the expansion medium was supplemented with 10 μM Y-27632 (Abmole, M1817). During culturing, medium was refreshed at most every three days. Images of organoid cultures were taken on EVOS FL Cell Imaging System (Thermo Fisher scientific). When specified, cell viability was determined using CellTiterGlo 3D (Promega) according to the manufacturer's instructions. Luminescence was acquired with Spark multimode microplate reader (Tecan).

Functional swelling assay

Functional swelling of human organoids was performed with established organoid lines (> passage 5). Organoids were mechanically split as usual at a ratio of 1:3 in expansion medium. After 2 days, the expansion medium was replaced with human differentiation medium for 8 days. Organoids became denser. For compound exposure, the human differentiation medium was freshly supplemented with 1 μM FSK, 1 mM dbcAMP (Sigma, D0627), 100 μM NorEpinephrine (Sigma), 50 mM Carbachol (Sigma), 5 mM Pilocarpine (Sigma), 250 nM VIP (Sigma, V3628) or nothing (control). Individual organoids were imaged and followed using EVOS FL Auto 2 (Thermo Fisher scientific) for 4 hours after adding the compounds. For quantification, individual organoid diameter (n = 11 per experiment) was measured before and 4 hours after exposure using ImageJ. Swelling ratio was determined by normalizing to the diameter of the organoids before exposure.

CRISPR/Cas9-mediated Pax6 knockout

Guide RNA targeting mouse *Pax6* exon 4 (sgPax6: CCCGGCAGAAGATCGTAGAG) was cloned into the pSpCas9(BB)-2A-GFP (PX458) plasmid as described elsewhere (Ran et al., 2013). Murine organoids were mechanically dissociated into small pieces and electroporated with 10 μg plasmid using the NEPA21 electroporator (Nepagene) as previously described (Fujii et al., 2015). Electroporated cells were plated in BME and cultured in expansion medium. After 3 days cells were dissociated into a single cell suspension and GFP-positive cells were sorted out using the BD FACSAria (BD Biosciences). Single sorted cells that formed an organoid were picked and expanded as clonal organoid lines for further characterization. *Pax6* genotype was investigated by PCR (Pax6_F1: TCCAGTGGGCAGGTTCAAAT, Pax6_R1: GGAAGGGCACTCCCGTTTAT, Pax6_F2: ATCATAGACGCGCTCCTTCC, Pax6_R2: CA CAAGCGTGATGGATGCAA). If evidence was found for genomic disruption around the sgRNA targeting region the organoid was further characterized for Pax6 protein using imaging and western blot.

Western blot

Organoids were collected from the BME using cold Cell Recovery Solution (Corning) for 30 min at 4°C. Total protein extract was isolated using RIPA Buffer (50 mM Tris-HCl pH 8.0, 150 mM NaCl, 0.1% SDS, 0.5% Na-Deoxycholate, 1% NP-40, 1X Complete protease inhibitors [Roche]) and the protein extract was sonicated. Samples were prepared for gel loading by measuring the concentration with a Bradford Assay (Bio-rad reagent). Samples were loaded on a pre-cast gradient SDS-PAGE gel 12% (Biorad) and run for 1-2 h at 100 V, for subsequent transfer onto a PVDF membrane (Millipore) overnight at 100 mA and at 4°C.

Membrane was blocked with 5% milk in PBST for 1 hour prior to incubation with primary antibody. Antibodies were rabbit anti-Pax6 (1:1000, Biolegend 901301) and goat anti-Hsp90 (1:1000, Origene TA500494) as a loading control. Secondary antibodies used were swine anti-rabbit-HRP (1:1000, Dako) and rabbit anti-goat/HRP (1:1000, Dako). After washing with PBS, revealing of the membrane was performed by exposing it to a mixture of 500 μL of Luminol and 500 μL of Peroxide (Western blot detection reagent kit, GE Healthcare) and imaged using ImageQuant LAS 4000 ECL western blot imager.

Immunohistochemistry and imaging

Organoids were harvested in cell recovery solution (354253, Corning) and fixed in 4% paraformaldehyde (Sigma-Aldrich) for at least 2 hours at room temperature. Lacrimal gland tissue used for immunohistochemistry was directly embedded in 4% paraformaldehyde upon dissection and fixed for at least 2 hours at room temperature. Samples were washed and dehydrated by an increasing ethanol gradient and washed in xylene before embedding in paraffin. Sections were cut and hydrated before staining. Hematoxylin and eosin (H&E) and Picro-Sirius red collagen stainings (Sigma) on organoids and tissue was performed as previously described (Sato et al., 2009) or according to the manufacturer's instructions. Antibody stainings on paraffin sections included human nucleolar marker (Abcam, ab-190710), PAX6 (Biolegend, 901301), AQP5 (Origene, TA307525), LTF (Millipore 07-685), KRT5 (clone AF138, Covance, 905501), KI67 (eBiosciences, 14-5698-82), ACTA2 (Sigma, A5228), LYZ (Dako, A0099), LCN2 (R&D systems, AF1757), BPIFA1 (Thermo Fisher Scientific, PA5-42187), PRR27 (Thermo Fisher Scientific, PA5-57546), WFDC2 (LSBio, LS-C175346), SCGB2A1 (Atlas antibodies, HPA034584), HTN1 (mybiosource, MBS2002621) and LCN1 (Santa Cruz Biotech, sc-374620) and were performed according to manufacturer's instructions. Slides were imaged using a Leica DM4000 microscope.

For immunofluorescence, organoids were harvested, fixed and permeabilized using 0.2% Triton X-100. Whole-mount staining was performed overnight in 2% donkey serum using the following reagents: anti-Pax6 (Biolegend, 901301), anti-Lcn2 (R&D systems AF1757), anti-AQP5 (Origene TA307525), anti-TP63 (Abcam, ab735), anti-KI67 (eBiosciences, 14-5698-82), Phalloidin–Atto 647N

Please cite this article in press as: Bannier-Hélaouët et al., Exploring the human lacrimal gland using organoids and single-cell sequencing, Cell Stem Cell (2021), https://doi.org/10.1016/j.stem.2021.02.024

(1:5000, Sigma-Aldrich) and DAPI (Invitrogen). Secondary antibodies included Alexa Fluor 568 donkey anti-rabbit IgG (Life Technologies, A10042) and Alexa Fluor 568 donkey anti-goat IgG (Life Technologies, A11057). Organoids were imaged on a Leica SP8X or SP8 microscope.

qPCR analysis

RNA isolations of organoids and tissue for bulk RNA sequencing and qPCR were performed with RNeasy Mini Kit (QIAGEN) following the manufacturer's instructions. Quantitative PCR analysis was performed using the SYBR Green and Bio-Rad systems. Changes in expression relative to house keeping gene and lacrimal gland tissue when indicated were calculated using CFX manager software (Bio-Rad). Primers were designed using NCBI primer design tool and are indicated in Table S5.

Bulk mRNA sequencing

Bulk mRNA sequencing was performed by the Utrecht Sequencing Facility (USEQ) using the TruSeq stranded mRNA kit (Illumina). In short, polyA enriched RNA was reverse transcribed and paired-end reads mapped to the mouse genome. Expression data was analyzed using DESeq2 (Love et al., 2014). GO term enrichment analysis was performed using the goseq package (Young et al., 2010). To plot the expression of human tear proteome genes, genes were retrieved from Supplemental Data 3 of a previous publication (Dor et al., 2019).

Single-cell mRNA sequencing

For single-cell sequencing of the tissue, human lacrimal gland was dissociated with collagenase I (Sigma-Aldrich) as described above and subsequently resuspended in TrypLE Express (GIBCO) pre-heated to 37°C and dissociated under repeated pipetting. For single-cell sequencing of the organoids, organoid droplets were incubated with dispase (3:400, Thermo Fisher Scientific) for 30 minutes in order to dissolve the BME. Then, organoids were pelleted and incubated in Accutase (Thermo Fisher scientific) supplemented with 10 μM Y-27632 (Abmole, M1817) in a water bath at 37°C for at least 20 minutes. When the gland and the organoids were fully dissociated into single cells, samples were pelleted, washed, resuspended in FACS buffer (advanced DMEM/F12, 10 μM Y-27632 and DAPI) and strained (35 μm).

DAPI-negative cells were immediately sorted into 384-well plates containing ERCC spike-ins (Agilent), RT primers and dNTPs (Promega) using a BD FACSJazz, FACSAriaII, FACSFusion or FACSMelody (all BD Biosciences). Plates were prepared using Mosquito HTS (TTPlabtech). Single-cell RNA sequencing libraries were prepared following the SORT-seq protocol (Muraro et al., 2016), which is based on the CEL-seq2 method (Grün et al., 2015). In short, cells were first lysed for 5 minutes at 65 °C, and RT and second-strand mixes were dispensed by the Nanodrop II liquid handling platform (GC Biotech). Single-cell double-stranded cDNAs were pooled together and *in vitro* transcribed for linear amplification. Illumina sequencing libraries were prepared using the TruSeq small RNA primers (Illumina) and these DNA libraries were sequenced paired-end, respectively, on the Illumina NextSeq.

Bioinformatics analysis

Fastq files were trimmed with TrimGalore-0.4.3 and mapped with STAR-2.5.3a to the human reference genome (GRCh38). Introns and exons were extracted from the corresponding annotation files. Cells with raw transcript counts higher than 1.5 times the interquartile range above the upper quartile of the rest of the population were removed as potential doublets. Subsequently, clustering and single-cell analysis were performed with RaceID3 (Herman et al., 2018) using the following parameters: mintrans = 4000 for the organoids and mintrans = 1500 for the tissue, knn = NULL, cln = NULL, clusternr = 30, probthr = 1e-3, perplex = 30.

To directly compare organoid and tissue cells in the violin plots, cells identified in the above-mentionned analysis were retrieved from another analysis containing both tissue and organoid cells ran with mintrans = 1500. Then, normalized expression (ndata) was plotted.

For RNA velocity analysis the filtered expression data from RaceID3 was processed with the scVelo package according to a previous publication (Bergen et al., 2020) with following parameters: min_shared_counts = 10, n_top_genes = 2000, n_pcs = 30, n_neighbors = 10 using a dynamical model. Velocity was depicted using the dynamic stream embedding function of the scVelo package. All bioinformatics analysis was performed using R version 3.6.1 (R Foundation, https://www.r-project.org) and Python 3.6.5 (https://www.python.org/).

Organoid transplantation

Human lacrimal gland organoids were split as normally. 3 days after splitting, BME was removed using dispase (Thermo Fisher scientific) as described above, organoids were harvested and resuspended in human expansion medium supplemented with 5% BME.

Then, NSG mice were sedated using isoflurane. About 5 μL of organoid suspension (~150,000 cells) was directly injected into each mouse lacrimal gland using an insulin needle. After 2 weeks, 1 month and 2 months, mice were sacrificed and their lacrimal glands were harvested for immunohistochemistry analysis of the engraftment. A total of 4 mice (i.e., 8 lacrimal glands) were injected per time point.

Please cite this article in press as: Bannier-Hélaouët et al., Exploring the human lacrimal gland using organoids and single-cell sequencing, Cell Stem Cell (2021), https://doi.org/10.1016/j.stem.2021.02.024

Statistical analysis

No statistical method was used beforehand to determine sample size. The investigators were not blinded and no data points was excluded. Data is represented as mean ± standard error to the mean. The number of duplicates as well as the type of test performed is indicated in each figure legend.